Early-orogenic deformation in the Ionian zone of the Hellenides: Effects of slab retreat and arching on syn-orogenic stress evolution

S. Tavani[a,*], A. Corradetti[b], M. De Matteis[c], A. Iannace[a], S. Mazzoli[a], A. Castelluccio[d], D. Spanos[e], M. Parente[a]

[a] Dipartimento di Scienze della Terra, dell'Ambiente e delle Risorse, Università Federico II, Naples, Italy
[b] Department of Petroleum Engineering, Texas A&M University at Qatar, Qatar
[c] Dipartimento di Scienze della Terra "A. Desio", Università degli studi di Milano, Milan, Italy
[d] Edison, Milan, Italy
[e] Hellenic Petroleum, Maroussi, Greece

ARTICLE INFO

Keywords:
Fractures
Thrust and fold belt
Greece
Orocline

ABSTRACT

In this work we report on early-orogenic fracture patterns affecting a Cretaceous to Eocene sedimentary succession exposed in western Greece. These rocks belong to the Cenozoic External Hellenides, which form the western portion of the Aegean orocline. The analysis of fracture type, orientation, and crosscutting relationships provides constraints on the stress and strain patterns during the early stages of orocline formation. The fracture patterns in the study area includes early-orogenic extensional fractures arranged into two mutually orthogonal sets. These developed during progressive burial in the forebulge-foredeep system, ahead of the advancing compressive front. Tectonic solution seams at a high angle to bedding postdate these extensional structures. Solution seams are arranged in different sets, oblique to each other, and developed in the early stages of thrusting and folding. Extensional structures and solution seams are oblique to each other. Their orientation and crosscutting relationships provide evidence for clockwise vertical axis rotation of stress directions with time. This is consistent with the progressive arching of the forebulge-thrust belt system during progressive slab retreat.

1. Introduction

Curved belts are ubiquitous and occur across different scales in both ancient and active orogenic systems (e.g. Eldredge et al., 1985; Marshak, 1988, 2004; Silver et al., 1990; Cunningham, 1993; Speranza et al., 1997; Weil et al., 2000, 2013; Mazzoli et al., 2001, 2005; Weil and Sussman, 2004; Allmendinger et al., 2005; Cifelli et al., 2008; Johnston and Mazzoli, 2009; Cawood et al., 2011; Gutiérrez-Alonso et al., 2011; Mattei et al., 2017; Szaniawski et al., 2017). Oroclines constitute a particular class of curved belts, in which folding in map view occurs by buckling or bending of an initially almost linear belt (e.g. Carey, 1955; Marshak, 2004). Many challenging geological issues are associated with orocline formation, among which the evolution in time and space of stress and strain patterns has received great attention (e.g. Ries and Shackleton, 1976; Pastor-Galán et al., 2011). Linear fold-and-thrust belts, indeed, are characterised by a rather simple evolution of the stress field. As described in Tavani et al. (2015) (Fig. 1a), in linear belts the onset of convergence is marked by belt-perpendicular extension in the forebulge/foredeep region, followed by belt-parallel extension in the foredeep. Later on, shortening occurs ahead and within the thrust wedge, with the shortening direction being oriented perpendicular to the belt and almost parallel to bedding (i.e. layer parallel shortening, LPS). In agreement, the stress history of linear belts in the early stage of the orogenic process involves permutations among the stress tensor axes. The directions of these axes remain essentially constant, being oriented either parallel or perpendicular to the trend of the belt, and almost perpendicular to bedding (Tavani et al., 2015 and references therein). During orocline development, progressive arching adds complexities to such a simple history (Fig. 1b). Arching requires lateral strain, such as outer-arc extension and inner-arc compression in map view. For instance, this strain pattern produces belt-parallel extension and compression components in the frontal and inner portions of the orocline, respectively (e.g. Gutiérrez-Alonso et al., 2012). Such a strain pattern is well depicted by syn-orocline meso-structures in secondary arcs (i.e. that developed in response to buckling or bending of a pre-existing linear belt). More complex strain patterns can instead be produced in progressive arcs. There, orocline formation occurs synchronously with folding and thrusting (Fig. 1b and c), and rotations of

* Corresponding author.
E-mail address: stefano.tavani@unina.it (S. Tavani).

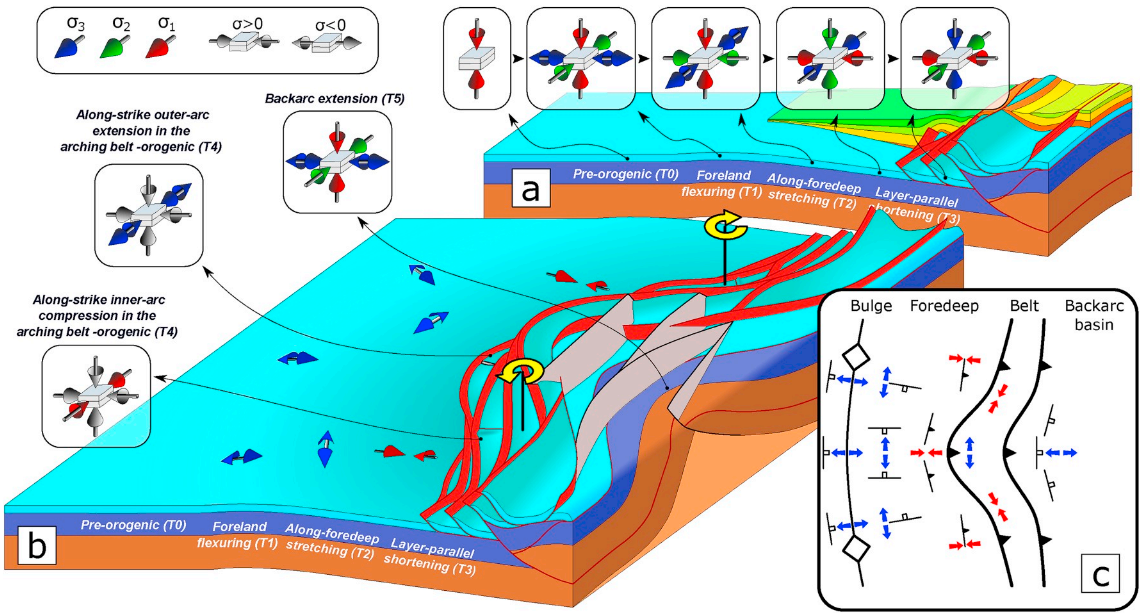

Fig. 1. Stress in fold and thrust belts. 3D schemes showing the architecture of linear (a) and curved (b) foreland fold-and-thrust belts and the typical evolution of the stress field during the early orogenic stages. (c) Map view of a curved belt with expected directions of extension (blue arrows) and compression (red arrows). (For interpretation of the references to colour in this figure legend, the reader is referred to the Web version of this article.)

both blocks and stress axes occur.

Coeval arching and thrust belt development has occurred in the Aegean orocline (Jolivet et al., 2013; Rosenbaum, 2014). There, ongoing slab retreat is considered the causative process for orocline formation and for coeval back-arc extension in the Aegean Sea (e.g. Jolivet et al., 2013 and references therein). Moreover, paleomagnetic studies in the area pointed out how vertical axis rotation occurred synchronously with thrusting and folding (e.g. Broadley et al., 2006).

In this work we present a meso-structural study in the Ionian fold and thrust belt of Greece. This constitutes the external portion of the western side of the Aegean Orocline. By this work we intend to: (i) show the effect of trench retreat and arching on fracture network development, and (ii) demonstrate the reliability of fracture data in constraining geodynamic processes. Early works proposed that fracture distribution in thrust and fold belts mostly relates with the shape of the hosting thrust-related anticlines (e.g. Stearns, 1968). However, more recent studies have indicated that pre-thrusting and pre-folding processes are more important in determining the fracture pattern in fold and thrust belts (Geiser and Sansone, 1981; Dunne and North, 1990; Railsback and Andrews, 1995; Lash and Engelder, 2007; Quintà and Tavani, 2012; Beaudoin et al., 2012 Weil and Yonkee, 2012; Arboit et al., 2015; Branellec et al., 2015; Korneva et al., 2016; Rustichelli et al., 2016). On the other hand, these later studies, as well as tens of other works in similar and different tectonic settings (e.g. Engelder and Geiser, 1980; Hancock, 1991; Rawnsley et al., 1998; Eyal et al., 2001; Pastor-Galán et al., 2011; Lamarche et al., 2012; Izquierdo-Llavall et al., 2013; Savignano et al., 2016; Beaudoin and Lacombe, 2018; Tavani et al., 2018) have demonstrated the reliability of meso-structures (e.g. striated meso-faults, joints, veins, and solution seams) in constraining the paleo-stress fields over large areas. The present work has been developed in the framework of the documented link between fracture pattern and geodynamic processes. We used orientation, angular relationships with bedding and overprinting relationships of joints, veins, solution seams, and meso-faults, measured in different sites, to define the early-orogenic fracture pattern of the region. Our results provide new constraints on the evolving stress field during foreland lithosphere bending and associated extension, and during the subsequent layer parallel shortening stage of this orocline.

2. Geological setting

The Hellenides constitute the southern portion of the roughly NW-trending Dinarides-Albanides-Hellenides belt (Fig. 2a). This developed due to the Cenozoic collision between the Adria-Africa and Eurasian continental paleomargins (e.g. Dercourt et al., 1986; Dewey et al., 1973; Aubouin et al., 1976, Robertson and Shallo, 2000; Roure et al., 2004; Papanikolaou, 2009), after the subduction of the oceanic basins originally interposed between them (e.g. Robertson and Dixon, 1984; Robertson et al., 1991; Saccani et al., 2003; Bortolotti et al., 2013). Active subduction is presently occurring in the southernmost portion of the orogenic system, where the Ionian lithosphere is underthrusting northward below the Eurasian one (e.g. McKenzie, 1972, 1978; Spakman et al., 1988; Underhill, 1989). The active trench is located along the southern border of the arched Mediterranean ridge accretionary complex (e.g. Le Pichon et al., 1982). The transition from subduction to continental collision occurs along the NNE-SSW striking, seismically active Kefalonia right-lateral transform fault (e.g. Louvari et al., 1999; Sachpazi et al., 2000; Pearce et al., 2012) (Fig. 2b and c). Arching of the trench occurred progressively since the late Miocene and led to the formation of the so-called Aegean Orocline (e.g. Pastor-Galán et al., 2017). This is characterised by counterclockwise vertical-axis rotations in the eastern Aegean area (Kissel and Poisson, 1987; Morris and Robertson, 1993; van Hinsbergen et al., 2010) and clockwise vertical axis rotations (of up to 90°) in the different domains of the Albanides (e.g. Speranza et al., 1995) and Hellenides (e.g. Laj et al., 1982; Kondopoulou, 2000; van Hinsbergen et al., 2005, 2006; Broadley et al., 2006) (Fig. 2b).

The study area is located in the Ionian zone of the External Hellenides (Fig. 2b). This area is separated from the Internal Hellenides by a suture zone involving relics of the Mesozoic Pindos Ocean, formerly dividing the Apulian (Adria-Africa) and Pelagonian (Europe) crustal blocks (e.g. Smith et al., 1979; Mountrakis, 1986; Jones and Robertson, 1991; Doutsos et al., 1993). In detail, the External Hellenides fold and thrust belt is constituted by NNW elongated thrust-bounded zones where the Meso-Cenozoic sedimentary successions of different palaeographic domains are exposed (e.g. Aubouin, 1965; Jenkins, 1972; Underhill, 1988, 1989; Karakitsios, 1995). These domains, developed onto the Adria plate during the Early Jurassic rifting,

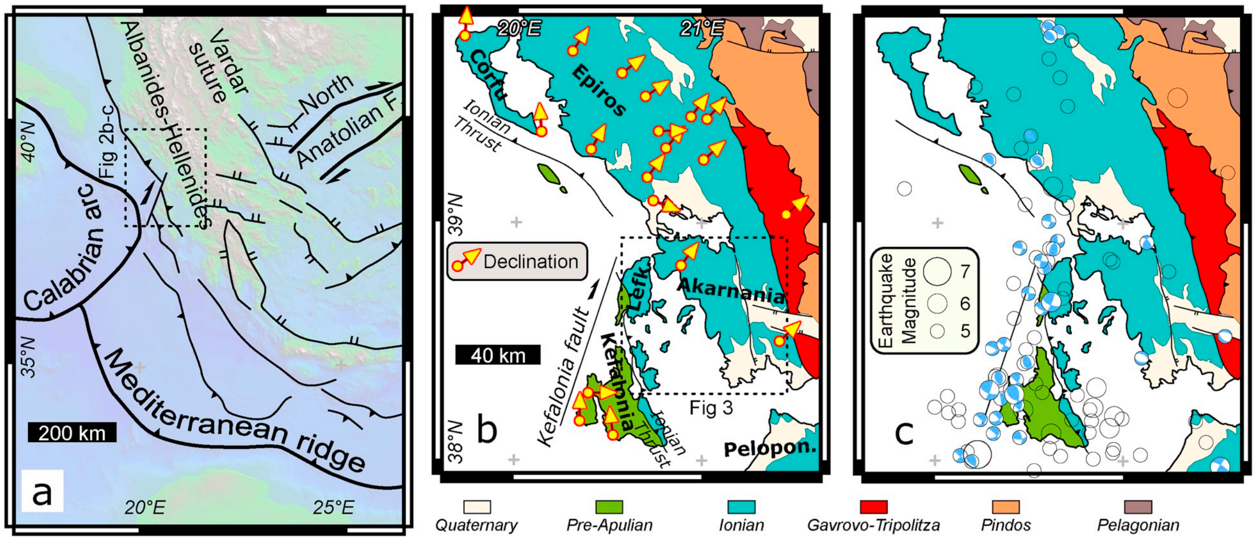

Fig. 2. The Hellenides. (A) Structural scheme of the Albanides-Hellenides and surrounding areas (after Jolivet et al., 2013). Geological map of the External Hellenides (after Broadley et al., 2006), with (B) paleodeclinations (data from van Hinsbergen et al., 2005) and (C) *Mw* > 5 earthquake distribution (source USGS, https://earthquake.usgs.gov/).

are from west (foreland) to east (hinterland) (e.g. Aubouin, 1965; Smith et al., 1979; Robertson et al., 1991; Karakitsios, 1995, 2013): (i) The Apulian carbonate platform (located to the west of the area in Fig. 2b); (ii) the pre-Apulian or Paxos zone (Fig. 2b), consisting of Triassic to Miocene neritic and pelagic carbonates; (iii) the Ionian pelagic basin; and (iv) the Gavrovo-Tripolitza carbonate platform, passing eastward to the Pindos oceanic basin. Thrusting in the Hellenides roughly evolved in a piggy-back sequence, from east to west (Smith and Moores, 1974; Robertson and Dixon, 1984), although out-of-sequence thrusting is also locally documented (e.g. Sotiropoulos et al., 2003). During the late Eocene the terrains of the Pindos ocean were thrusted westward (Degnan and Robertson, 1998, Skourlis and Doutsos, 2003; Doutsos et al., 2006). Since then, flexural subsidence established in the Gavrovo and Ionian zones. During the Oligocene and the Miocene, the foredeep-thrust belt system progressively migrated forelandward (i.e. westward). Thrusting progressively affected the Gavrovo, Ionian, and pre-Apulian zones, resulting in the development of the External Hellenides fold and thrust belt (Aubouin et al., 1976; Underhill, 1989; Doutsos et al. 2006). The external portion of the fold and thrust belt is still undergoing active compression (Kiratzi and Louvari, 2003; Jolivet et al., 2013). This is shown by earthquakes indicating right-lateral motion along NNE-SSW striking faults (belonging to the Kefalonia fault system) and reverse slip along NW-SE to N-S striking faults (Fig. 2c). The forelandward migration of the belt-foredeep system was coeval with clockwise vertical axis rotation, which occurred in the External Hellenides since the middle Miocene (e.g. Duermeijer et al., 1999). More in detail, clockwise rotation of the External Hellenides occurred into two stages: the first one is middle to late Miocene in age and implied a rotation of about 30°–40°; the second stage, which started during the Quaternary, caused an additional rotation of up to 20° (e.g. Duermeijer et al., 1999; Broadley et al., 2006). The amount of rotation decreases forelandward (Broadley et al., 2006) (Figs. 2b and 3), being less than 20° in the Corfu and Ithaki islands immediately to the east of the Ionian Thrust. Complex rotation patterns are instead observed in Kefalonia and Lefkada islands (Figs. 2b and 3), and have been interpreted as related to the Kefalonia right-lateral fault (Birch, 1994).

The Ionian zone, where we collected fracture data, includes large parts of some Ionian islands (i.e. Corfu, and large sectors of Ithaki and Lefkada), the Epiros, the Akarnania, the western part of Peloponnesus and the southern portion of Albania (Figs. 2b and 3). It is bounded to the west by the NW-SE to NNW-SSE striking Ionian thrust, having the pre-Apulian zone in its footwall, and to the east by the NNW-SSE striking Gavrovo thrust. The Ionian zone in the study area can be further subdivided into a western and an eastern area, separated by the NNW-SSE striking Katouna-Stamna fault system (Fig. 3). This is an active left-lateral transtensive fault system (Pérouse et al., 2017) that developed after the main thrusting and folding stage. To the east of this fault system, Cenozoic strata are largely exposed (with small areas where Jurassic and Cretaceous rocks crop out) and structures are homogeneously NNW-SSE-oriented. To the west of the Katouna-Stamna fault system, instead, the entire Triassic to Quaternary multilayer crops out and different structural trends occur. In detail, thrusts and folds are primarily NNW-SSE oriented, coherently with the WSW-ENE oriented shortening recognised in the area (e.g. Underhill, 1989), but some oblique folds also occur. Some of these oblique trends can be framed within the 3D architecture of NNW-SSE striking faults (e.g. lateral ramps). However, others indicate different shortening directions. These include the E-W striking folds located immediately to the east of the Lefkada Island (which record N-S shortening).

The sedimentary succession of the Ionian zone is divided into three major sequences (Karakitsios, 1995): (i) the Triassic-Sinemurian pre-rift sequence, (ii) the Pliensbachian-Tithonian syn-rift sequence, and (iii) the Tithonian-Eocene post-rift sequence, capped by late Eocene (Priabonian) - Oligocene Flysch strata (IGRS-IFP, 1966) (Fig. 3). The pre-rift sequence starts with poorly exposed Middle Triassic evaporites (IGRS-IFP, 1966), overlain by Ladinian-Carnian bituminous limestones and Norian dolostones (the Foustapidima Limestone Fm.; Renz, 1955; Karakitsios and Tsaila-Monopolis, 1990). It ends with the Lower Jurassic (Hettangian to Sinemurian) thick-bedded to massive shallow-water carbonates of the Pantokrator Limestone Formation (Renz, 1955; Flügel, 1983; Karakitsios and Tsaila-Monopolis, 1988). The overlying syn-rift strata contain Middle to Upper Jurassic hemipelagic limestones and marls that were deposited as asymmetric wedges associated with listric block faulting (Siniais Limestone Formation and Louros Limestone Formation, followed by the "Posidonia beds" and laterally equivalent Ammonitico Rosso Formation and Limestone with Filaments Formation; Bernoulli and Renz, 1970; Karakitsios, 1993). These strata mark the progressive deepening of the entire Ionian domain and the change from carbonate platform to deep-water basinal facies (Karakitsios, 1995, 2013). They are capped by the post-rift sequence, which directly overlies remnants of up-faulted blocks of the Pantokrator Limestone Formation in some cases. The post-rift sequence consists of

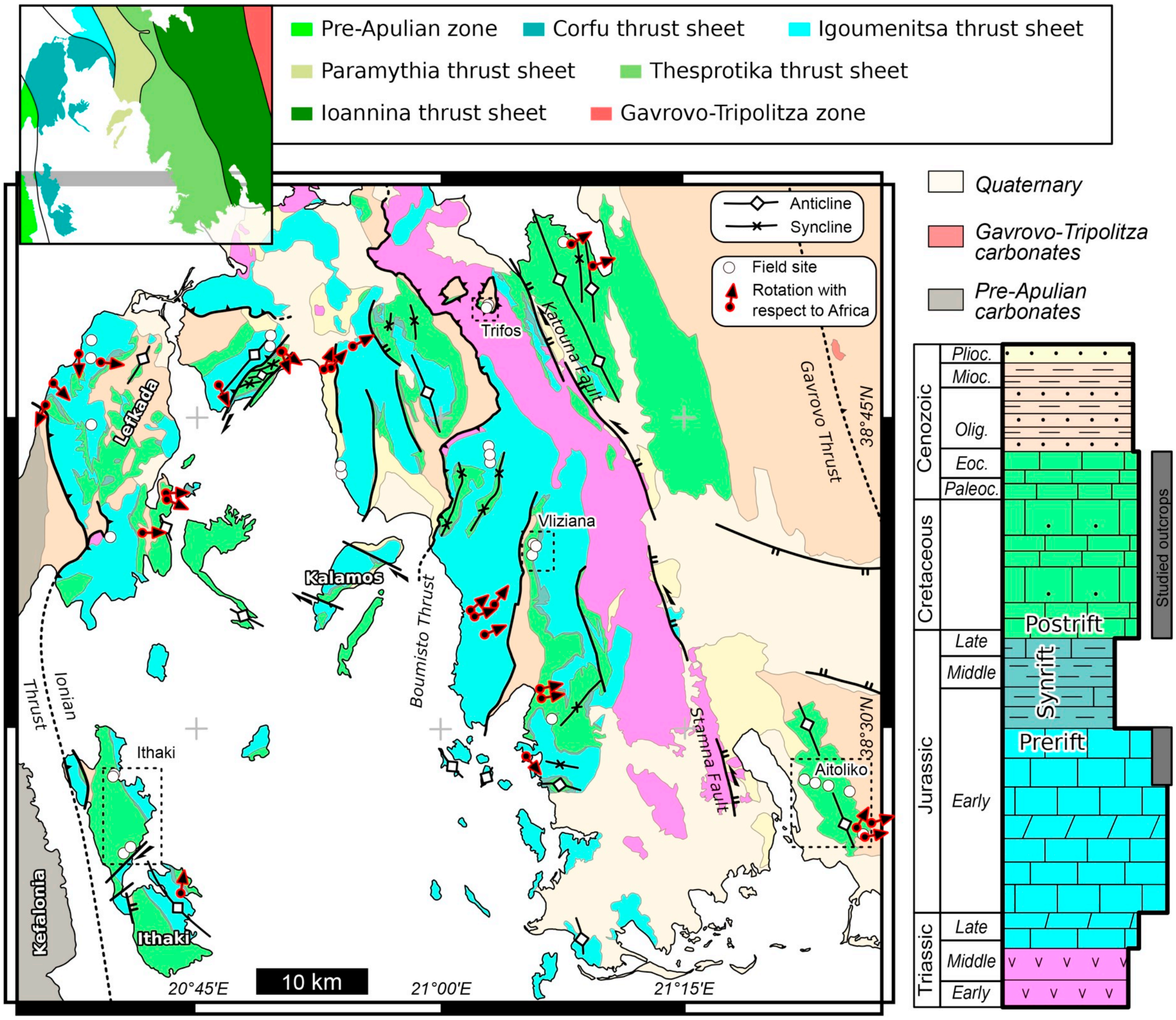

Fig. 3. The Ionian Zone. Geological map and stratigraphy of the Ionian zone, with field measurement sites and structural scheme of major thrust sheets (after Broadley et al., 2006). Arrows indicate rotations relative to fixed Africa (after Broadley et al., 2006).

uppermost Jurassic-Lower Cretaceous chert-bearing deep-water limestones, called Vigla Limestone Formation (Aubouin, 1959; IGRS-IFP, 1966; Skourtsis-Coroneou et al., 1995; Danelian et al., 1997). These are overlain by Upper Cretaceous to Eocene pelagic and hemipelagic limestones interlayered with frequent calcareous re-sediments, which have been called with different informal names (e.g.: Calcaire microbrechique and Calcaire sublithographique formations, IGRS-IFP, 1966; Microbreccious Limestone Formation, Karakitsios, 1995; Senonian Limestone and Microbreccious Limestone formations, Karakitsios and Rigakis, 2007). The Eocene pelagic limestones make a gradual transition to the overlying so-called Ionian Flysch Unit. The transition, generally occurring over an interval less than 20 m thick, is marked by the progressive increase of marly interlayers, followed by the appearance of the first siliciclastic beds (Fleury, 1980; Kamberis et al., 2005; Sotiropoulos et al., 2008).

3. Fracture data

Data of meso-faults, joints, veins, and pressure solution seams (excluding the bedding parallel ones) affecting Jurassic to Eocene formations have been measured in 27 field sites (Fig. 3). These sites are located in different thrust sheets of the Ionian belt and have been deformed at shallow crustal levels (i.e. at a maximum depth of 2–3 km). Meso-structures (in the following referred to as fractures) have been characterised in terms of type, orientation, and abutting/crosscutting relationships. Opening mode fractures have been classified in the field into veins and joints based on the occurrence or absence of visible cement infill, respectively. In agreement, joints include barren joints but also some veins with extremely thin (or weathered and removed) cement film (e.g. Laubach, 2003; Ukar et al., 2019). However, this is not a critical point for our study. Indeed, veins and joints in the studied outcrops are mutually exclusive structures (characterised by the same orientations, as illustrated below). Veins occur together with abundant bedding-parallel stylolites (most likely supplying calcite for vein infilling), whereas joints are mostly found in sites with scarce bedding-parallel stylolites. The reference bedding has also been measured, and fracture data are displayed both in present-day orientation and after restoring the bedding to the horizontal.

3.1. Fracture types

3.1.1. Joints

In their present-day orientation, irrespectively of their structural and stratigraphic locations, joints are clustered into four major sets. Two of them include near vertical surfaces striking NE-SW and NW-SE. The other two sets include N- and S-dipping surfaces (Fig. 4). Clustering of joints increases in the unfolded projection, where joints are near vertical (i.e. bedding-perpendicular) and NE-SW and NW-SE striking.

3.1.2. Veins

Veins are characterised by a similar pattern as joints, both in the present-day orientation and after unfolding. In detail, when bedding dip is removed, veins are clustered into two broad sets including bedding-perpendicular structures striking NW-SE and, secondarily, NE-SW.

3.1.3. Solution seams

Pressure solution seams are clustered in various sets in present-day orientation, the major one being sub-vertical and E-W striking. In the unfolded setting, solution seams are organised into two near vertical (i.e. bedding-perpendicular), roughly E-W and N-S striking sets.

3.1.4. Faults

The measured fault planes are steeply dipping and NW-SE striking (Fig. 4). When bedding dip is removed, faults become clustered into two, NE-SW and NW-SE striking sets at a high angle to bedding. The plot of rotaxes (i.e. the slip-normal direction along the fault plane; Salvini and Vittori, 1982) of normal faults indicates roughly E-W extension (i.e. N-S trending rotaxes) along W-dipping faults. When bedding dip is removed, the direction of extension provided by rotaxes of normal faults becomes WNW-ESE. Rotaxes of reverse faults indicate, particularly for the unfolded dataset, NNW-SSE oriented reverse motion along WSW-ENE striking faults and E-W oriented reverse movements (N-S trending rotaxes) along N-S striking faults. Slickenlines of strike-slip faults, both in present-day orientation and after bedding dip removal, are not well clustered. Only the WNW-ESE striking left-lateral strike-slip fault set can be clearly identified.

3.2. Fractures in the different structural domains

To better define fracture pattern development during the post-rift stage, fracture data collected in the Jurassic portion of the multilayer have been removed. This has been done to rule out all fractures that possibly developed during or immediately after the Jurassic rifting event, even though these fractures could have played a role during the subsequent phases. The remaining fracture data have been collected in the Cretaceous to Eocene pelagic and hemipelagic limestones interlayered with calcareous re-sediments of four areas (Fig. 3). These areas correspond to different structural domains of the Ionian belt that, from the innermost to the outermost, are: (*i*) a broad area near the Aitoliko town, characterised by gently dipping bedding, located to the east of the Stamna fault; (*ii*) the upright frontal limb of an anticline close to the Vliziana village, located in the hanging wall of the Boumisto thrust; (*iii*) a NE-dipping limb exposed at the Trifos tectonic window, in the footwall of the Boumisto thrust; (*iv*) a synclinal area exposed at the Ithaki island, in the hanging wall of the Ionian thrust. Available paleomagnetic data (e.g. van Hinsbergen et al., 2005; Broadley et al., 2006) suggest nearly 60° of post Eocene clockwise rotation for the Aitoliko and Vliziana areas and less than 20° of clockwise rotation for the Ithaki sites. For the Trifos site we took into account the 40–60° post-Eocene clockwise rotation measured in the surrounding area (Fig. 3).

Bedding and fracture data collected in these four areas are presented in Fig. 5. Fractures are displayed in their unfolded attitude; joint and vein datasets have been merged, due to their identical pattern in the cumulative analysis. The correctness of considering together veins and joints is also supported by the observation that they are mutually exclusive, as mentioned above.

3.2.1. Aitoliko area

Fracture data in the Aitoliko sites have been collected in sub horizontal to gently N-dipping strata of the Ioannina thrust sheet. Both joints and veins occur in this area. They are bedding perpendicular and are clustered into two main maxima - roughly mutually orthogonal - corresponding to N80° and N178° striking fractures (Fig. 5). The pressure solution seams in the Aitoliko sites are bedding-orthogonal and define at least three maxima, corresponding to surfaces striking N58°, N113°, and N177°. Faults in the Aitoliko sites are rather scattered. The rotaxes of normal faults are N-S to NNE-SSW trending, recording E-W extension. The rotaxes of reverse faults are mostly NE-SW trending, i.e. parallel to the main trend of the solution seams, indicating NW-SE shortening, with a few additional elements mostly E-W striking. Slickenlines of right-lateral strike-slip faults in the Aitoliko sites are NW-SE trending, whereas those of left-lateral faults are both NE-SW and WNW-ESE trending.

3.2.2. Vliziana area

The Vliziana sites are located in the Thesprotika thrust sheet. Bedding surfaces in the Vliziana sites are WNW-dipping (Fig. 5), with bedding dip ranging from 60° to 90°. Both joints and veins occur in the Vliziana area; they are bedding-perpendicular and show a main strike of N121°. Solution seams are bedding-perpendicular and have a main strike of N13°; they form a mean angle of 108° with the main joint/vein set. Faults are both NW-SE and NE-SW striking. The rotaxes of normal faults indicate both NE-SW and NW-SE oriented extension, while the rotaxes of reverse faults indicate WNW-ESE oriented shortening.

3.2.3. Trifos area

The Trifos area corresponds to a tectonic window in the Paramythia thrust sheet, where the footwall of the Boumisto thrust is exposed. In the Trifos sites, strata are NE-dipping, with an average dip of 50°. Similarly to the Aitoliko sites, in the Trifos sites joints and veins are arranged into two bedding-perpendicular sets striking N27° and N106°, respectively, and thus forming an angle of nearly 80°. The solution seams are bedding-perpendicular too and strike N95°; they are neither parallel nor perpendicular to both joint/vein sets. E-W striking faults are at a high angle to bedding and frequently display normal offset (as detailed below), whereas the WSW-striking and 40° dipping faults are characterised by a reverse kinematics, as indicated by E-W trending rotaxes of reverse faults.

3.2.4. Ithaki area

The last of the four areas is the Ithaki island, forming part of the Corfu thrust sheet, where we collected fracture data both from sub-horizontal and steeply SW-dipping strata. Both joints and veins occur in the Ithaki area. These structures are bedding-perpendicular and organised into two sets displaying mean strike of N1° and N115°, respectively. Solution seams are at a high angle to bedding and their strike is rather scattered, with a main set of N61° striking surfaces. Faults are roughly WNW-ESE striking and 70° dipping toward the SSW. Although no kinematic indicators have been measured along these faults, the stratigraphic offsets after bedding dip removal are mostly normal.

3.3. Relative chronology of fractures

Abutting/crosscutting relationships between the different fracture sets have been observed and carefully evaluated. Bedding-perpendicular veins and some extensional faults striking parallel to them show opposite crosscutting relationships with bedding-parallel stylolites. In many cases veins postdate the stylolites (Fig. 6a) (n = 22 observations) but in others bedding-parallel stylolites clearly truncate, and thus postdate, veins (Fig. 6b and c) (n = 15 observations). E-W striking extensional faults observed at the Trifos sites frequently show evidence of an early-diagenetic origin. This is documented, for example, by ductile deformation observed in cherty layers (Fig. 7a), indicating that the chert was not yet completely lithified during extensional faulting. Additional evidence is provided by extensional faulting accommodated by en-echelon veins, with the veins being coeval with bedding-parallel stylolites (Fig. 7b). The occurrence of closely-spaced bedding-parallel stylolites is generally associated with the occurrence of bedding-perpendicular veins, in which the dissolved calcite is precipitated. Indeed, where bedding-parallel stylolites are rare, the calcite infill is rare too and joints are observed instead of veins with the same structural trend (Fig. 7c). As seen in the cumulative contour plot of joints/veins and

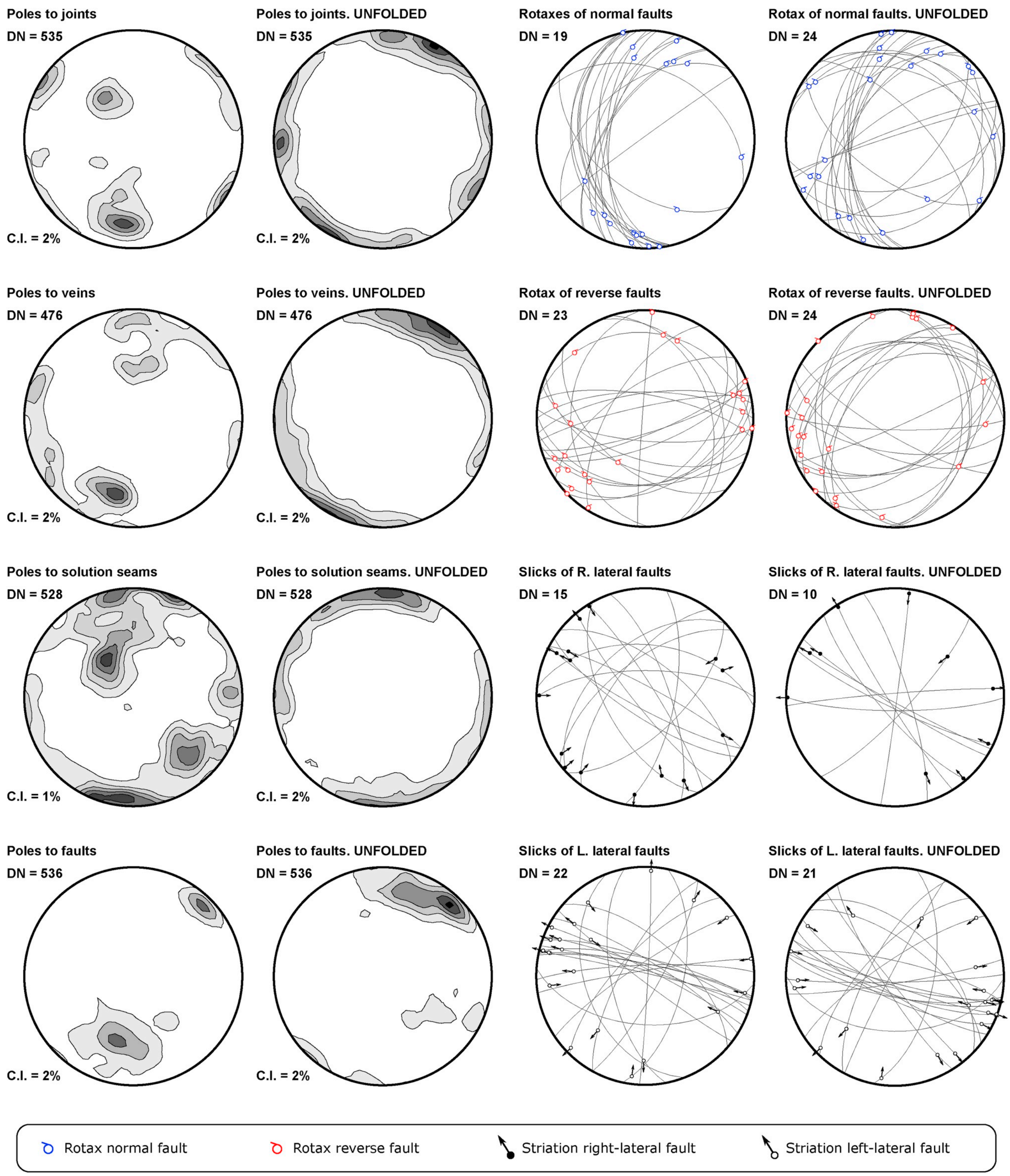

Fig. 4. Fracture data. Cumulative density contour of poles to joints, veins, solution seams, and faults, and stereoplots of faults with striations or rotaxes (i.e. slip-normal) indicated. Data are displayed both in the present-day orientation and after bedding dip removal. Here and in the following, plots are in stereographic lower hemisphere projection.

solution seams in the four areas (Fig. 5), solution seams are oblique to the joints and veins. Solution seams are either at a high (Figs. 7c, 8a and 8c) or at a low angle (Fig. 8b and c) with the joint/vein sets and only locally we have observed bedding-perpendicular veins oriented perpendicular to the solution seams (Fig. 9a). In most of the cases (n = 25 observations), solution seams truncate (i.e. postdate) the joint/vein sets (Fig. 8), and only in a limited suite of outcrops (n = 2 observations) we have observed bedding-perpendicular veins post-dating the solution seams. In the Vliziana and Trifos sites, solution seams are characterised by a single bedding-perpendicular set, striking (after bedding dip removal) NNE-SSW and E-W, respectively. On the other hand, in the Aitoliko and Ithaki sites, solution seams are still at a high angle to bedding but they are organised in multiple sets. In the Aitoliko area, we have observed N-S oriented teeth along the oblique junction zones between N-S and E-W striking solution seams (Fig. 9a). In the same area, N-S striking solution seams are crosscut and displaced by E-W

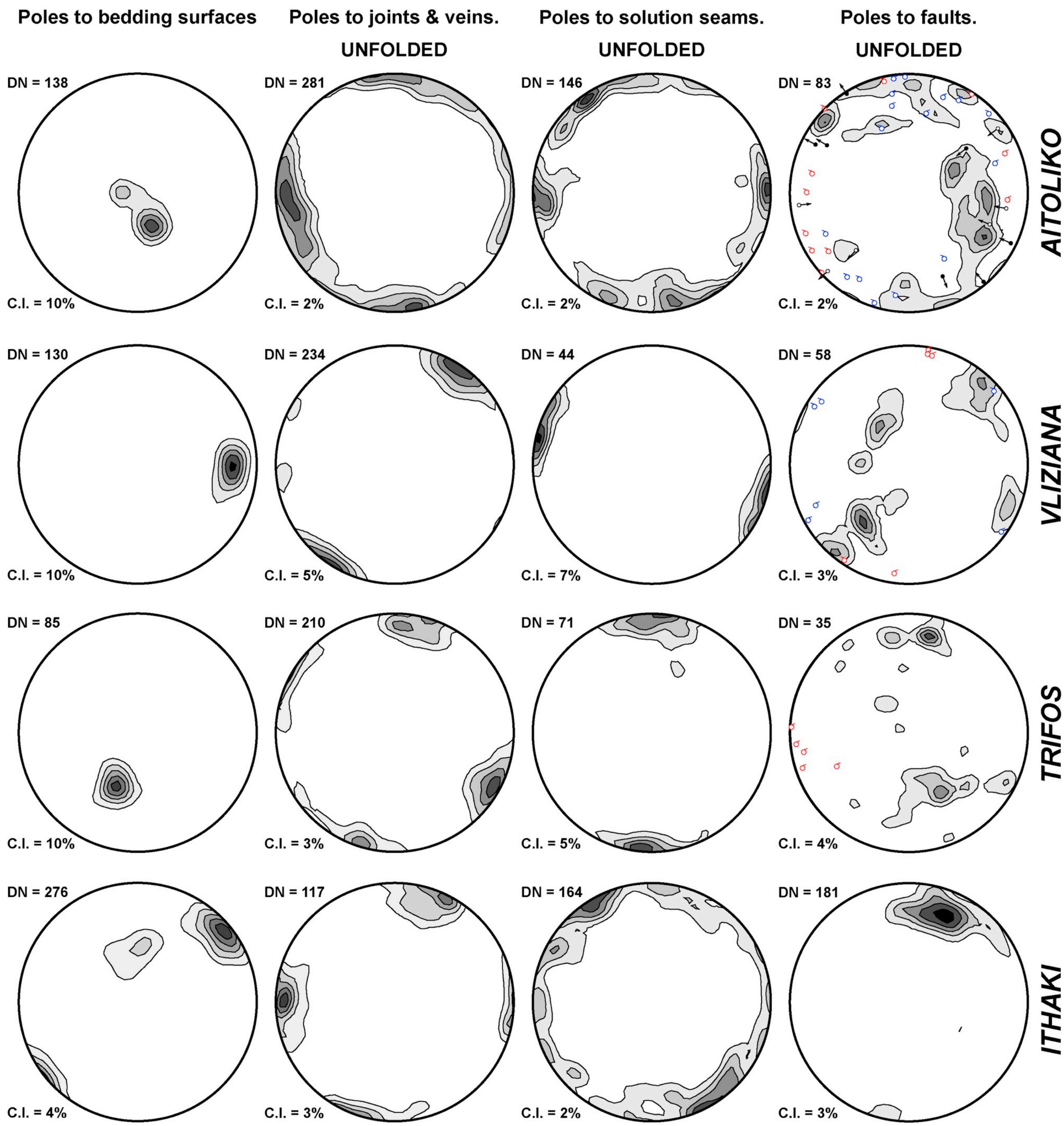

Fig. 5. Fracture data in the Cretaceous to Eocene units. Cumulative density contour of poles to bedding, joints and veins, solution seams, and faults in the Vliziana, Aitoliko, Trifos, and Ithaki areas (see Fig. 2 for location). Faults, joints and veins, and solution seams are displayed after bedding dip removal. Rotaxes and striations are included in the plot of faults (see Fig. 3 for colour codes). (For interpretation of the references to colour in this figure legend, the reader is referred to the Web version of this article.)

striking seams (Fig. 9b). Both types of observations (for a total of five sites) indicate how, in the Aitoliko sites, N-S shortening postdates E-W shortening. A similar observation is made close to the Vliziana sites. As already mentioned, in the Cretaceous to Eocene multilayer of these sites, only one set of bedding-perpendicular solution seams occurs. However, a few kilometres to the west, in Lower Jurassic limestones, both N-S and E-W striking sets of solution seams occur. There, the E-W striking set postdates the N-S striking set, as indicated by strongly oblique N-S trending stylolitic teeth found along the N-S striking solution seams (Fig. 9c). In the Trifos sites, only one set of solution seam is documented, whereas in the Ithaki sites the E-W striking bedding-perpendicular solution seams again postdate the N-S striking seams (Fig. 9d) (four observations).

4. Discussion

4.1. Fracture assemblages and timing

4.1.1. Extensional fractures

The study area is characterised by the occurrence of bedding-perpendicular veins and fractures, which are oriented almost parallel to high-angle extensional faults, postdated by multiple sets of bedding-

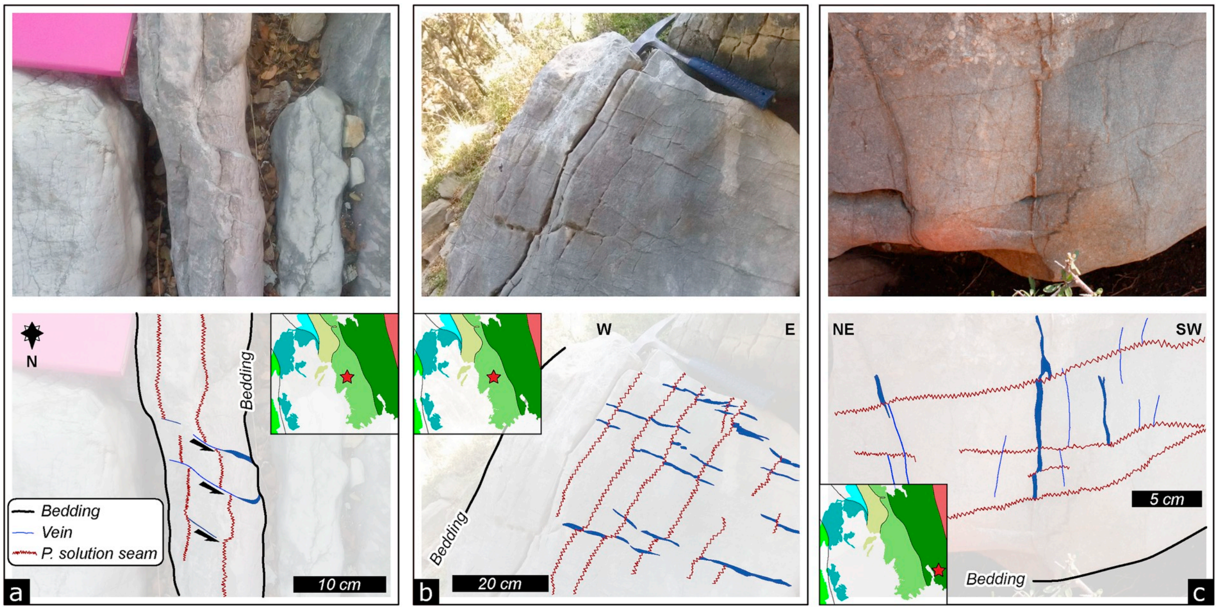

Fig. 6. Pre-to early-orogenic meso-structures. (A) View from above of a near-vertical bed in the Vigla Fm. hosting tilted small-scale normal faults coeval with bedding-parallel stylolites. Vliziana area. (B) Steeply W-dipping strata of the Vigla Fm., exposing bedding-perpendicular veins displaced by bedding-parallel stylolites. Vliziana area. (C) Sub-horizontal Cretaceous limestones with bedding-perpendicular veins displaced by bedding-parallel stylolites. Aitoliko area.

perpendicular solution seams. In many tectonic settings, joints and veins developed at different burial conditions (e.g. Gillespie et al., 2001). In the study area, instead, we have observed that: (*i*) joints and veins have identical trends; (*ii*) they are mutually exclusive, i.e. either veins or joints are found in a single outcrop; (*iii*) outcrops at short distance (< 10 m) from each other are either joints or veins dominated; (*iv*) veins occur where pressure solution seams are abundant. These observations indicate that joints and veins formed during the same tectonic stages, but in rock volumes where abundant dissolved calcite supplied by solution seams was circulating and re-precipitating (veins) or not (joints). The cumulative contouring of extensional structures shows that NNE-SSW and WNW-ESE striking structures (Fig. 4), when grouped by area, increase their clustering and define two (roughly) mutually orthogonal sets (Fig. 5), oriented neither parallel nor perpendicular to the strike of local bedding, nor to the trend of the hosting anticlines (as seen in Fig. 3). Many of these structures clearly show a syn-burial origin, coeval with bedding-parallel solution seams (Figs. 6 and 7a,b), so it is assumed that they have a pre-to early-orogenic origin.

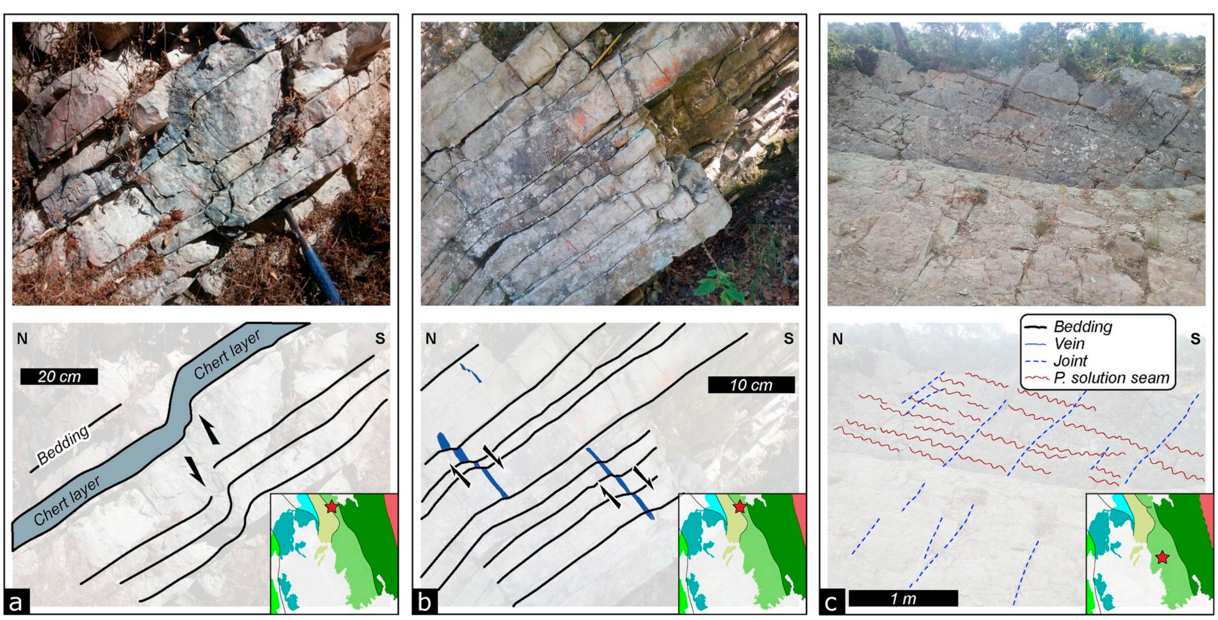

Fig. 7. Pre-to early-orogenic meso-structures. (A) Tilted normal fault in N-dipping strata of the Vigla Fm. The fault arrests on a cherty layer, which is coherently folded, evidencing a ductile deformation of silica and thus an early-diagenetic character of the fault. Trifos area. (B) Tilted normal faults in N-dipping strata of the Vigla Fm. These faults are formed by en-echelon bedding-perpendicular veins, which are displaced by bedding-parallel stylolites (forming the bed boundaries in this exposure), in turn folded by the incipient faulting, these relationships indicating faulting during burial and bedding-parallel stylolites development. Trifos area. (C) Frontal view of the steeply W-dipping upper Eocene strata just below the transition with the Flysch deposits, hosting bedding perpendicular joints predating bedding-perpendicular solution seam (which abut on them). Vliziana area. Joints are oriented parallel to veins occurring a few strata below.

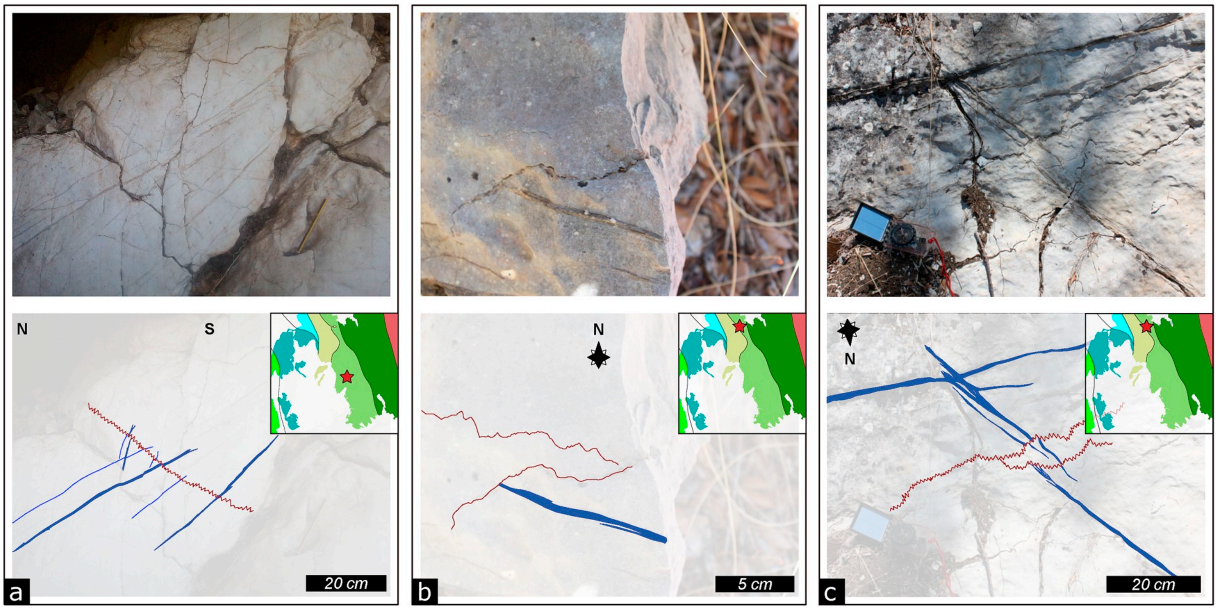

Fig. 8. Crosscutting relationships between veins and bedding-perpendicular solution seams. (A) Frontal view of a S-dipping limestone bed of the Vigla Fm., showing a NNE-SSW striking (after unfolded) bedding-perpendicular solution seam displacing NW-SE striking (after unfolding) veins. Vliziana area. (B) View from above of a gently N-dipping Eocene limestone bed hosting an E-W striking bedding perpendicular solution seam consuming the tip area of - thus postdating – a E-W striking bedding perpendicular vein. Trifos area. (C) View from above of sub-horizontal Eocene limestone beds, with nearly E-W striking solution seams displacing N-S striking veins. Trifos area.

Graham Wall et al. (2006) and Lacombe et al. (2009) documented identical structures in the Albanides, a few hundreds of kilometres to the NW of our study area. These authors attributed the formation of bedding-perpendicular veins and bedding-parallel solution-seams to the overburden stress during burial. More in detail, Lacombe et al. (2009) proposed that this association formed under a well-defined NNE-SSW directed extension before folding, in response to the flexuring of the lithosphere ahead of the advancing thrust sheets. This interpretation is in line with fracture studies in other fold and thrust belts worldwide (e.g. Ahmadhadi et al., 2008; Beaudoin et al., 2012; Carminati et al., 2014; Branellec et al., 2015; Hernández and Franzese, 2017; La Bruna et al., 2018; Tavani et al., 2018), suggesting how early-orogenic extensional structures that developed ahead of the belt frequently form a relevant portion of the fracture network affecting sedimentary rocks exposed in those fold and thrust belts. This network of extensional structures includes, like in the study area (e.g. Dunne and North, 1990; Laubach et al., 1998), two orthogonal sets. In particular, flexuring in the forebulge and along-foredeep stretching cause extension in the directions both parallel and perpendicular to the foredeep-belt system (Fig. 1) (e.g. Doglioni, 1995; Quintà and Tavani, 2012; Tavani et al., 2015), which fits with the occurrence of two orthogonal sets of extensional structures in the different sites of our study area.

4.1.2. Layer parallel shortening events

Based on crosscutting relationships, we suggest that early-orogenic extensional structures predate the layer-parallel shortening pattern, as documented also in the Albanides (Graham Wall et al., 2006; Lacombe et al., 2009), where the shortening direction is well clustered and oriented almost perpendicular to the strike of the belt (Lacombe et al., 2009). In the Ionian zone, where we carried out our meso-structural study, solution seams are organised in different sets, oblique to each other, and, together with reverse faults, define multiple layer-parallel shortening directions. Notably, bedding-perpendicular solution seams are not perpendicular to the veins (Fig. 5). Typically, the layer-parallel shortening pattern developing in linear fold and thrust belts includes mutually orthogonal bedding-perpendicular solution seams and veins (e.g. Engelder and Geiser, 1980; Mitra and Yonkee, 1985; Railsback and Andrews, 1995; Tavarnelli, 1997; Evans and Elmore, 2006; Tavani et al., 2012; Weil and Yonkee, 2012), with the veins corresponding to both newly formed structures oriented normal to the minimum acting stress (e.g. Fletcher and Pollard, 1981) and re-opened joints inherited from the early orogenic stages (e.g. Gratier et al., 2005; Tavani et al., 2015). In linear belts, these two types of veins (i.e. newly formed and re-opened) are almost indistinguishable, as the minimum stress directions during along-foredeep stretching and layer-parallel shortening stages coincide (Fig. 1). In the study area, due to the curved shape of the belt, solution seams and veins are not mutually perpendicular. This observation, together with the crosscutting relationships between these elements, indicate the occurrence of vertical axis rotations of either the stress field or crustal blocks (or both) during the transition from along-foredeep stretching to layer-parallel shortening stages. Concerning the origin of the layer-parallel shortening patterns, it must be taken into account that most bedding-perpendicular solution seams are mostly almost parallel to the trend of the belt. However, additional sets also occur, oriented oblique to the trend of the belt. The (almost) belt-parallel solution seams are abundant (except for the Trifos site) and their occurrence is in line with belt-perpendicular, E-W oriented shortening. Such an E-W oriented shortening is also consistent with the earthquake pattern of western Greece, indicating that active E-W horizontal compression is occurring immediately to the west of the study area (e.g. Clément et al., 2000). However, in between the E-W shortening event in the study area and the present-day E-W oriented active shortening affecting the external portion of the Hellenides, a N-S shortening event has occurred. This is indicated by widespread, roughly E-W striking solution seams postdating the N-S striking solution seams (Figs. 9b and 10). More in detail, the different sets of bedding-perpendicular pressure solution seams are not exactly perpendicular, allowing us to discard the stress permutation mechanism (e.g. Zhou and Aydin, 2012) as the causative process for the development of multiple generations of solution seams. This obliquity, together with the occurrence of some E-W trending folds and NW-SE striking left-lateral faults (Fig. 3), points to a N-S oriented, belt-parallel, shortening event postdating the main E-W shortening event (and thus the development of N-S trending major thrust-related anticlines). Actually, the solution seam pattern is even

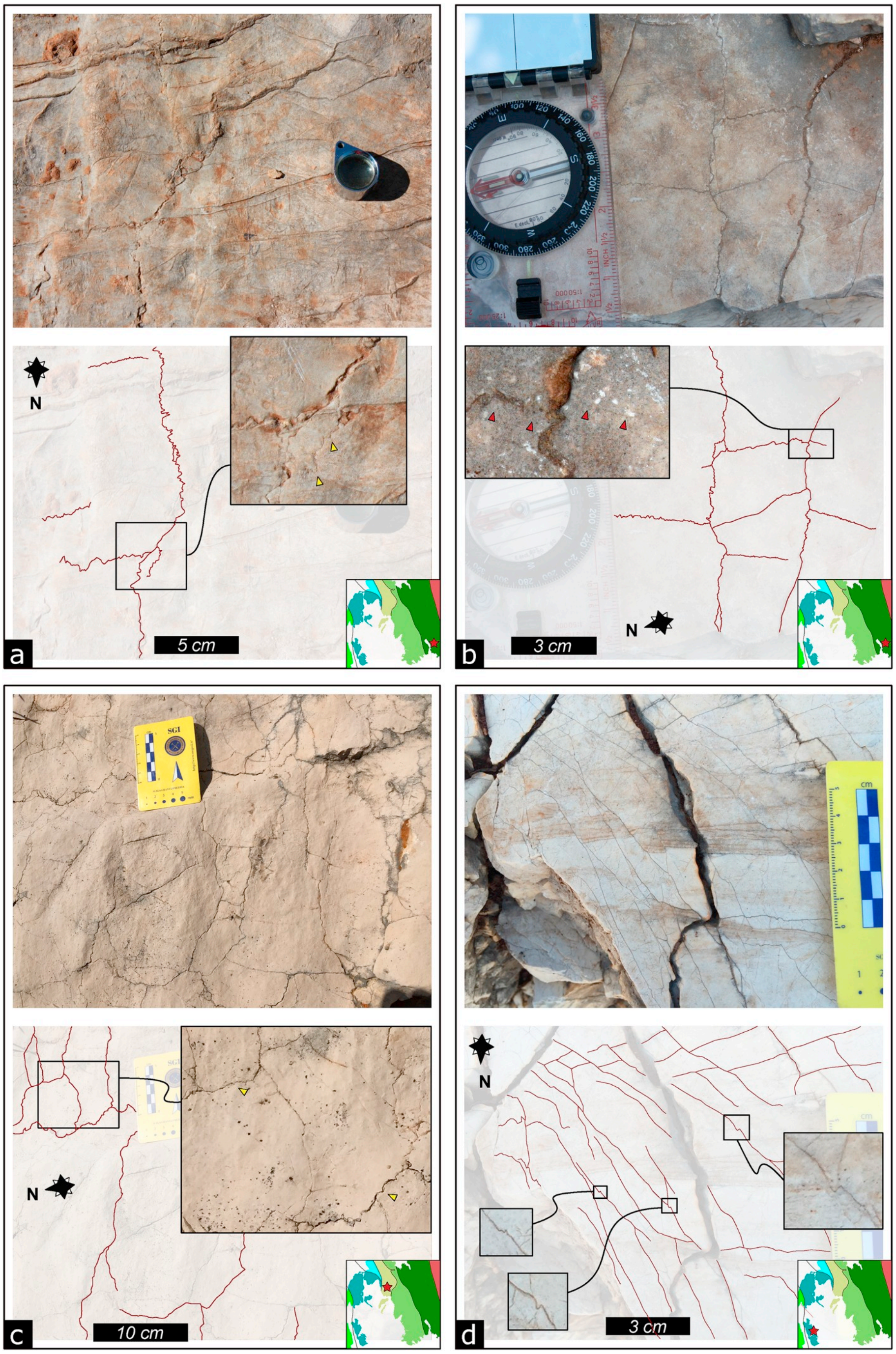

Fig. 9. Crosscutting relationships between bedding-perpendicular solution seam sets. Views from above of sub-horizontal limestone beds exposing E-W striking bedding perpendicular solution seams post-dating N-S striking bedding perpendicular seams. (A) The relative timing between the two sets is visible in the junction zone, where the teeth are N-S trending, thus indicating that N-S oriented shortening postdate E-W oriented shortening. Cretaceous limestone, Aitoliko area. (B) E-W striking solution seams offset the N-S seams, whose displaced segments on the opposite walls of the E-W seams are still recognisable. Cretaceous limestone, Aitoliko area. (C) The occurrence of N-S trending teeth along the N-S striking solution seams evidence that N-S oriented shortening postdate E-W oriented shortening. Jurassic limestone, Mitikas area (about 15 km west of the Vliziana area). (D) N-S trending teeth along NNW-SSE striking solution seams evidence that the last stage of shortening was N-S oriented. Eocene limestone, Ithaki.

more complex, as belt-perpendicular shortening affects areas that have undergone variable vertical axis rotations.

4.2. *Fracture pattern development and thrust belt evolution*

To better understand the stress evolution during the early stages of the orogenic process, Fig. 10 shows directions of extensional structures and solution seams in the present-day orientation. The figure also shows the pre-vertical axis rotation shortening directions, as derived from the orientation of solution seams (i.e. the directions orthogonal to the solution seam sets and parallel to their teeth) and the trend of the forebulge-foredeep as derived from extensional structures (i.e. parallel or orthogonal to the joint/vein sets). In order to display the data in the pre-vertical axis rotation reference frame, the data from the Aitoliko, Vliziana, and Trifos sites have been rotated 60° counterclockwise, removing the vertical axis rotation with respect to the Ithaki site. Sites are sorted from the innermost (Aitoliko) to the outermost (Ithaki). The results show a progressive forelandward clockwise rotation of the trend of the forebulge-foredeep system and of both first and second layer-parallel shortening events. The age of foredeep infill in this portion of the Ionian fold and thrust belt is late Eocene-Miocene (IGRS-IFP, 1966; Bellas, 1997; Sotiropoulos et al., 2008; Triantaphyllou, 2013), whereas vertical axis rotation (VAR) started since the middle Miocene, as indicated by paleomagnetic studies (e.g. Duermeijer et al., 1999). Accordingly, extension in the forebulge predated VAR, whereas thrusting and folding and VAR were probably coeval, as suggested by Broadley et al. (2006). When Miocene to recent VARs are removed, we observe a forelandward rotation of the strike of the forebulge-foredeep-related

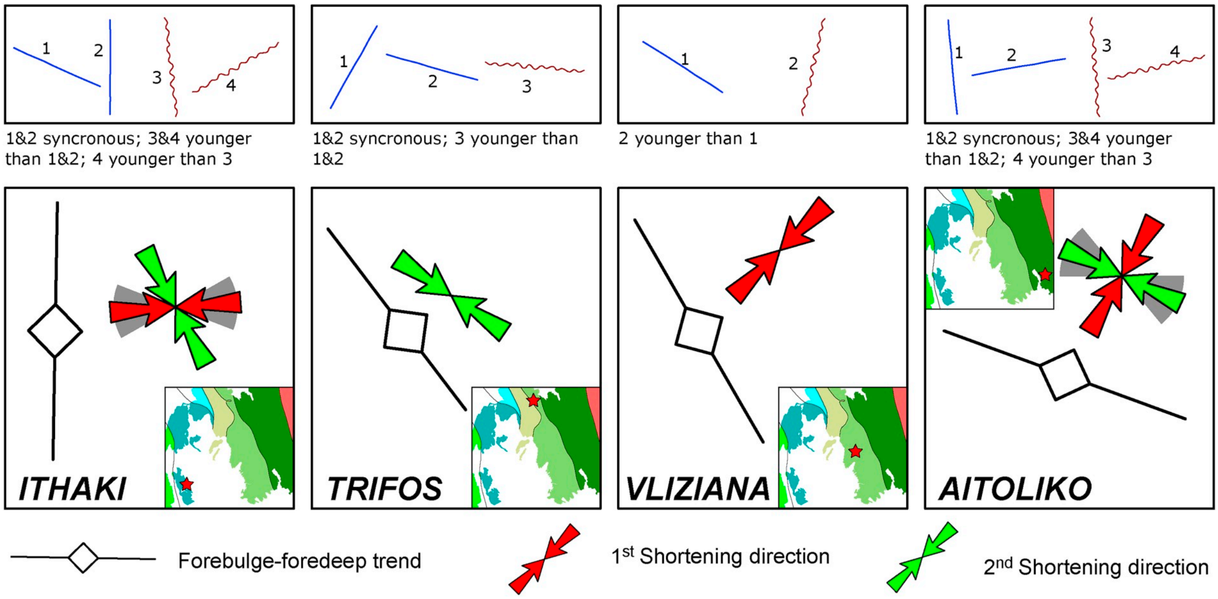

Fig. 10. Forebulge and LPS directions. Map view (boxes on top) of extensional fractures (blue) and solution seams (red) in the four sites in their present day orientation, with summary of crosscutting relationships. Below, the forebulge-foredeep and layer parallel shortening directions inferred for the four studied sites, obtaining by removing vertical axis rotation and assuming that the forebulge-foredeep trend is parallel/perpendicular to the joint/vein sets. (For interpretation of the references to colour in this figure legend, the reader is referred to the Web version of this article.)

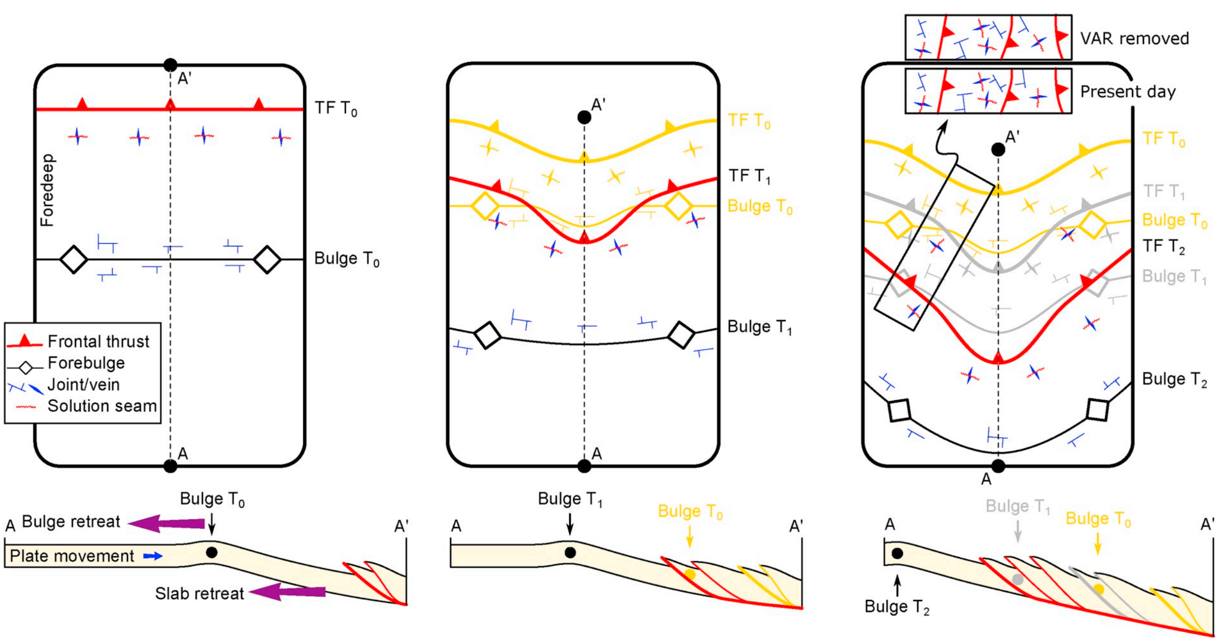

Fig. 11. Fracture pattern evolution during progressive slab and trench arching and retreat. Schemes showing, in map view and cross section, the effect of the progressive arching and retreat of the subducting slab and trench onto the fracture pattern, with the thrust front, forebulge, and fractures developed at each step being progressively rotated after their incorporation into the thrust belt.

extensional structures. This indicates the occurrence of a progressive arching, in map view, of the forebulge. Differential retreat of the subducting Ionian slab (e.g Jolivet et al., 2013) provides an explanation for this. Indeed, as illustrated in Fig. 11, differential slab retreat causes bulge and trench retreat, and their progressive arching as well. Arching - in map view - of the bulge was not accompanied by remarkable VAR. Vertical axis rotation and progressive arching occurred in the thrust sheets of the thrust belt, imposing a non-linear pattern to the layer parallel shortening directions ahead of the frontal thrust. Both extensional (bulge and foredeep-related) and shortening-related (i.e. solution seams associated with belt-orthogonal layer-parallel shortening) structures were then incorporated into the advancing fold and thrust belt, where they underwent VAR. Such a complex tectonic history, however, produced an apparently simple pattern. Indeed, the final (i.e. present day) orientation of both shortening-related and extensional structures is almost parallel (or perpendicular) to the present day local trend of the belt, regardless of the amount of VAR they underwent. An identical situation is documented in the transverse fold system of the Ainsa basin (Pyrenees), where along-belt compression and extension are suggested to be related to the arching of the belt (e.g.Vidal-Royo et al., 2009, Muñoz et al., 2013). In agreement, we deduce that along-belt shortening postdating belt-perpendicular shortening relates with a slight differential rotation, inducing inner arc compression in map view. As shown in the inset of Fig. 11, the present-day orientation of compressional and extensional structures of the Ionian zone is roughly parallel and perpendicular to the present-day trend of the foredeep-thrust belt system. However, removing VAR reveals that early-orogenic extension in the bulge-foredeep system and consequent layer-parallel shortening occurred during progressive slab and trench retreating and arching.

5. Conclusions

Despite having experienced a long and complex structural history, including folding and thrusting and late high-angle faulting, the studied Cretaceous to Eocene sedimentary succession of the External Hellenides of western Greece is characterised by a 'background' fracture network – including two joint sets orthogonal to each other – that appears to be associated with the early fault sets that formed during the first (forebulge-to foredeep-related) deformation stage ahead of the advancing thrust front. A spaced, disjunctive pressure-solution cleavage at a high angle to bedding postdates the early extensional structures. This pressure-solution cleavage, which developed in the early stages of thrusting and folding, includes different sets oblique to each other. Their orientation and crosscutting relationships with respect to early extensional joints and veins record clockwise vertical axis rotation of the stress field and arching of the belt from its innermost to outermost parts. Our model (Fig. 11) reconciles complex structural overprinting relationships with a relatively simple tectonic evolution involving progressive arching of the forebulge-thrust belt system during progressive slab retreat in the Aegean orocline.

Acknowledgements

Authors thank the Editor, S.E. Laubach, and two anonymous reviewers for their useful suggestions, which greatly improved the paper.

References

Ahmadhadi, F., Daniel, J.M., Azzizadeh, M., Lacombe, O., 2008. Evidence for pre-folding vein development in the Oligo-Miocene Asmari Formation in the central Zagros fold belt, Iran. Tectonics 27 (1), 1–22. https://doi.org/10.1029/2006TC001978.

Allmendinger, R.W., Smalley Jr., R., Bevis, M., Caprio, H., Brooks, B., 2005. Bending the Bolivian orocline in real time. Geology 33 (11), 905–908. https://doi.org/10.1130/G21779.1.

Arboit, F., Amrouch, K., Collins, A.S., King, R., Morley, C., 2015. Determination of the tectonic evolution from fractures, faults, and calcite twins on the southwestern margin of the Indochina Block. Tectonics 34 (8), 1576–1599. https://doi.org/10.1002/2015TC003876.

Aubouin, J., 1959. Contribution â l'étude géologique de la Grèce septentrionale: les confins de l'Epire et de la Thessalie. Ann. Geol. Des. Pays Hell. 10, 1–483.

Aubouin, J., 1965. Geosynclines. Elsevier Publ. Co., Amsterdam, pp. 335.

Aubouin, J., Bonneau, M., Davidson, J., Leboulenger, P., Matesco, S., Zambetakis, A., 1976. Esquisse structurale de l'arc egeen externe: des Dinarides aux Taurides. Bull. Soc. Geol. Fr. 18, 327–336.

Beaudoin, N., Lacombe, O., 2018. Recent and future trends in paleopiezometry in the diagenetic domain: insights into the tectonic paleostress and burial depth history of fold-and-thrust belts and sedimentary basins. J. Struct. Geol. 114, 357–365. https://doi.org/10.1016/j.jsg.2018.04.001.

Beaudoin, N., Leprêtre, R., Bellahsen, N., Lacombe, O., Amrouch, K., Callot, J.P., Emmanuel, L., Daniel, J.M., 2012. Structural and microstructural evolution of the rattlesnake mountain anticline (Wyoming, USA): new insights into the sevier and laramide orogenic stress build-up in the Bighorn basin. Tectonophysics 576, 20–45. https://doi.org/10.1016/j.tecto.2012.03.036.

Bellas, S., 1997. Calcareous nannofossils of the tertiary flysch (post Eocene to early Miocene) of the Ionian zone in Epirus, NW-Greece: taxonomy and biostratigraphical correlations. Berliner Geowissenshaftliche Abhandlungen 22, 1–173.

Bernoulli, D., Renz, O., 1970. Jurassic carbonate facies and new ammonite faunas from western Greece. Eclogae Geol. Helv. 63 (2), 573–607.

Birch, W., 1994. Palaeomagnetic Studies in Western and Central Greece: Tectonic Evolution of the Aegean Domain since the Triassic (Ph.D. thesis). Liverpool University.

Bortolotti, V., Chiari, M., Marroni, M., Pandolfi, L., Principi, G., Saccani, E., 2013. Geodynamic evolution of ophiolites from Albania and Greece (Dinaric-Hellenic belt): one, two, or more oceanic basins? Int. J. Earth Sci. 102 (3), 783–811. https://doi.org/10.1007/s00531-012-0835-7.

Branellec, M., Callot, J.P., Nivière, B., Ringenbach, J.C., 2015. The fracture network, a proxy for mesoscale deformation: constraints on layer parallel shortening history from the Malargüe fold and thrust belt, Argentina. Tectonics 34 (4), 623–647. https://doi.org/10.1002/2014TC003738.

Broadley, L., Platzman, E., Platt, J., Papanikolaou, M., Matthews, S., 2006. Paleomagnetism and the tectonic evolution of the Ionian zone, northwestern Greece. Geol. Soc. Am. Spec. Pap. 409, 137–155. https://doi.org/10.1130/2006.2409(08).

Carey, S.W., 1955. The orocline concept in geotectonics-Part I. In: Papers and Proceedings of the Royal Society of Tasmania, vol. 89. pp. 255–288.

Carminati, E., Aldega, L., Trippetta, F., Shaban, A., Narimani, H., Sherkati, S., 2014. Control of folding and faulting on fracturing in the Zagros (Iran): the Kuh-e-Sarbalesh anticline. J. Asian Earth Sci. 79, 400–414. https://doi.org/10.1016/j.jseaes.2013.10.018.

Cawood, P.A., Pisarevsky, S.A., Leitch, E.C., 2011. Unraveling the New England orocline, east Gondwana accretionary margin. Tectonics 30, TC5002. https://doi.org/10.1029/2011TC002864.

Cifelli, F., Mattei, M., Della Seta, M., 2008. Calabrian Arc oroclinal bending: the role of subduction. Tectonics 27, TC5002. https://doi.org/10.1029/2011TC002864.

Clément, C., Hirn, A., Charvis, P., Sachpazi, M., Marnelis, F., 2000. Seismic structure and the active Hellenic subduction in the Ionian islands. Tectonophysics 329 (1–4), 141–156. https://doi.org/10.1016/S0040-1951(00)00193-1.

Cunningham, W.D., 1993. Strike-slip faults in the southernmost Andes and the development of the Patagonian orocline. Tectonics 12 (1), 169–186. https://doi.org/10.1029/92TC01790.

Danelian, T., De Wever, P., Azéma, J., 1997. Palaeoceanographic significance of new and revised palaeontological datings for the onset of Vigla Limestone sedimentation in the Ionian zone of Greece. Geol. Mag. 134 (6), 869–872. https://doi.org/10.1017/S0016756897007553.

Degnan, P.J., Robertson, A.H.F., 1998. Mesozoic-early Tertiary passive margin evolution of the Pindos ocean (NW Peloponnese, Greece). Sediment. Geol. 117 (1–2), 33–70. https://doi.org/10.1016/S0037-0738(97)00113-9.

Dercourt, J., Zonenshain, L.P., Ricou, L.E., Kazmin, V.G., Le Pichon, X., Knipper, A.L., Grandjacquet, C., Sbortshikov, I.M., Geyssant, J., Lepvrier, C., Pechersky, D.H., Boulin, J., Sibuet, J.C., Savostin, L.A., Sorokhtin, O., Westphal, M., Bazhenov, M.L., Laver, J.P., Biju-Duval, B., 1986. Geological evolution of the Tethys belt from the Atlantic to the Pamirs since the Lias. Tectonophysics 123, 241–315. https://doi.org/10.1016/S0037-0738(97)00113-9.

Dewey, J.F., Pitman, W.C., Ryan, W.B.F., Bonnin, J., 1973. Plate tectonics and the evolution of the Alpine system. Geol. Soc. Am. Bull. 84 (10), 3137–3180. https://doi.org/10.1130/0016-7606(1973)84<3137:PTATEO>2.0.CO;2.

Doglioni, C., 1995. Geological remarks on the relationships between extension and convergent geodynamic settings. Tectonophysics 252 (1–4), 253–267. https://doi.org/10.1016/0040-1951(95)00087-9.

Doutsos, T., Pe-Piper, G., Boronkay, K.T., Koukouvelas, I., 1993. Kinematics of the central Hellenides. Tectonics 12 (4), 936–953. https://doi.org/10.1029/93TC00108.

Doutsos, T., Koukouvelas, I.K., Xypolias, P., 2006. A new orogenic model for the external Hellenides. Geol. Soc. Lond. Spec. Publ. 260 (1), 507–520. https://doi.org/10.1144/GSL.SP.2006.260.01.21.

Duermeijer, C.E., Krijgsman, W., Langereis, C.G., Meulenkamp, J.E., Triantaphyllou, M.V., Zachariasse, W.J., 1999. A Late Pleistocene clockwise rotation phase of Zakynthos (Greece) and implications for the evolution of the western Aegean arc. Earth Planet. Sci. Lett. 173 (3), 315–331. https://doi.org/10.1016/S0012-821X(99)00226-5.

Dunne, W.M., North, C.P., 1990. Orthogonal fracture systems at the limits of thrusting: an example from southwestern Wales. J. Struct. Geol. 12, 207–215. https://doi.org/10.1016/0191-8141(90)90005-J.

Eldredge, S., Bachtadse, V., Van der Voo, R., 1985. Paleomagnetism and the orocline hypothesis. Tectonophysics 119 (1–4), 153–179. https://doi.org/10.1016/0040-1951(85)90037-X.

Engelder, T., Geiser, P., 1980. On the use of regional joint sets as trajectories of paleostress fields during the development of the Appalachian Plateau, New York. J. Geophys. Res. Solid Earth 85 (B11), 6319–6341. https://doi.org/10.1029/JB085iB11p06319.

Evans, M.A., Elmore, R.D., 2006. Fluid control of localized mineral domains in limestone pressure solution structures. J. Struct. Geol. 28 (2), 284–301. https://doi.org/10.1016/j.jsg.2005.10.004.

Eyal, Y., Gross, M.R., Engelder, T., Becker, A., 2001. Joint development during fluctuation of the regional stress field in southern Israel. J. Struct. Geol. 23 (2–3), 279–296.

Fletcher, R.C., Pollard, D.D., 1981. Anticrack model for pressure solution surfaces. Geology 9 (9), 419–424. https://doi.org/10.1130/0091-7613(1981)9<419:AMFPSS>2.0.CO;2.

Fleury, J.J., 1980. Évolution d'une plateforme et d'un basin dans leur cadre alpin: les zones de Gavrovo–Tripolitze et du Pinde–Olonos. Société Géologique du Nord Spécial Publication 4, 1–651.

Flügel, E., 1983. Mikrofazies der Pantokrator-Kalke (Lias) von Korfu, Griechenland. Microfacies of the Pantokrator limestones (Liassic) from Korfu, Greece. Facies 8, 263–300. https://doi.org/10.1007/BF02536744.

Geiser, P.A., Sansone, S., 1981. Joints, microfractures, and the formation of solution cleavage in limestone. Geology 9, 280–285. https://doi.org/10.1130/0091-7613(1981)9<280:JMATFO>2.0.CO;2.

Gillespie, P.A., Walsh, J.J., Watterson, J., Bonson, C.G., Manzocchi, T., 2001. Scaling relationships of joint and vein arrays from the Burren, Co. Clare, Ireland. J. Struct. Geol. 23, 183–201. https://doi.org/10.1016/S0191-8141(00)00090-0.

Graham Wall, B.R., Girbacea, R., Mesonjesi, A., Aydin, A., 2006. Evolution of fracture and fault-controlled fluid pathways in carbonates of the Albanides fold-thrust belt. AAPG Bull. 90 (8), 1227–1249. https://doi.org/10.1306/03280604014.

Gratier, J.P., Muquet, L., Hassani, R., Renard, F., 2005. Experimental microstylolites in quartz and modeled application to natural stylolitic structures. J. Struct. Geol. 27, 89–100. https://doi.org/10.1016/j.jsg.2004.05.007.

Gutiérrez-Alonso, G., Murphy, J.B., Fernández-Suárez, J., Weil, A.B., Franco, M.P., Gonzalo, J.C., 2011. Lithospheric delamination in the core of Pangea: Sm-Nd insights from the Iberian mantle. Geology 39 (2), 155–158. https://doi.org/10.1130/G31468.1.

Gutiérrez-Alonso, G., Johnston, S.T., Weil, A.B., Pastor-Galán, D., Fernández-Suárez, J., 2012. Buckling an orogen: the Cantabrian orocline. GSA Today 22 (7), 4–9. https://doi.org/10.1130/GSATG141A.1.

Hancock, P.L., 1991. Determining contemporary stress directions from neotectonic joint systems. Phil. Trans. Roy. Soc. Lond. 337, 29–40.

Hernández, M., Franzese, J.R., 2017. The fracture patterns of the Tin Tin anticline: fracturing process during the foreland evolution in the Calchaquí Valley, northwestern Argentina. J. Struct. Geol. 96, 54–64. https://doi.org/10.1016/j.jsg.2017.01.011.

IGRS-IFP, 1966. Etude Géologique de L'Epire (Gréce Nord-Occidentale). Technip, pp. 306.

Izquierdo-Llavall, E., Aldega, L., Cantarelli, V., Corrado, S., Gil-Peña, I., Invernizzi, C., Casas, A.M., 2013. On the origin of cleavage in the Central Pyrenees: structural and paleo-thermal study. Tectonophysics 608, 303–318. https://doi.org/10.1016/j.tecto.2013.09.027.

Jenkins, D.A.L., 1972. Structural development of western Greece. AAPG Bull. 56 (1), 128–149.

Johnston, S.T., Mazzoli, S., 2009. The Calabrian orocline: buckling of a previously more linear orogen. Geol. Soc. Lond. Spec. Publ. 327 (1), 113–125. https://doi.org/10.1144/SP327.7.

Jolivet, L., Faccenna, C., Huet, B., Labrousse, L., Le Pourhiet, L., Lacombe, O., Lecomte, E., Burov, E., Denèle, Y., Brun, J.P., Philippon, M., Paul, A., Salaün, G., Karabulut, H., Piromallo, C., Monié, P., Gueydan, F., Okay, A.,I., Oberhänsli, R., Pourteau, A., Augier, R., Gadenne, L., Driussi, O., 2013. Aegean tectonics: strain localisation, slab tearing and trench retreat. Tectonophysics 597–598, 1–33. https://doi.org/10.1016/j.tecto.2012.06.011.

Jones, G., Robertson, A.H., 1991. Tectono-stratigraphy and evolution of the Mesozoic Pindos ophiolite and related units, northwestern Greece. J. Geol. Soc. 148 (2), 267–288. https://doi.org/10.1144/gsjgs.148.2.0267.

Kamberis, E., Pavlopoulos, A., Tsaila-Monopolis, S., Sotiropoulos, S., Ioakim, C., 2005. Deep-water sedimentation and paleogeography of foreland basins in the NW Peloponnese (Greece). Geol. Carpathica 56, 503–515.

Karakitsios, V., 1993. The synrift sedimentation during extensional faulting from Upper Lias to Malm period and the inversion Tectonics in Ionian zone of Epirus (Greece). Bull. Geol. Soc. Greece 26 (1), 215–243.

Karakitsios, V., 1995. The influence of structure and halokinesis on organic matter preservation and thrust system evolution in Ionian basin, northwestern Greece. AAPG Bull. 79, 960–980. https://doi.org/10.1306/8D2B2191-171E-11D7-8645000102C1865D.

Karakitsios, V., 2013. Western Greece and Ionian Sea petroleum systems. AAPG Bull. 97 (9), 1567–1595. https://doi.org/10.1306/02221312113.

Karakitsios, V., Rigakis, N., 2007. Evolution and petroleum potential of western Greece. J. Pet. Geol. 30 (3), 197–218. https://doi.org/10.1111/j.1747-5457.2007.00197.x.

Karakitsios, V., Tsaila-Monopolis, S., 1988. Données nouvelles sur les niveaux supérieurs (Lias inférieur-moyen) des Calcaires de Pantokrator (zone Ionienne moyenne, Epire, Grèce continentale). Description des Calcaires de Louros: Rev. Micropaleontol. 31 (1), 49–55.

Karakitsios, V., Tsaila-Monopolis, S., 1990. Données nouvelles sur les niveaux inférieurs (Trias supérieur) de la série calcaire ionienne en Epire (Grèce continentale). Conséquences stratigraphiques. Rev. Paleobiologie, Genève 9 (1), 139–147.

Kiratzi, A., Louvari, E., 2003. Focal mechanisms of shallow earthquakes in the Aegean Sea and the surrounding lands determined by waveform modelling: a new database. J. Geodyn. 36 (1–2), 251–274. https://doi.org/10.1016/S0264-3707(03)00050-4.

Kissel, C., Poisson, A., 1987. Étude paléomagnetique préliminaire des formations cénozoïques des Bey Daglari (Taurides occidentales, Turquie). Comptes rendus de l'Académie des sciences. Série 2, Mécanique, Physique, Chimie, Sciences de l'univers, Sciences de la Terre 304 (8), 343–348.

Kondopoulou, D., 2000. Palaeomagnetism in Greece: Cenozoic and Mesozoic components and their geodynamic implications. Tectonophysics 326 (1–2), 131–151. https://doi.org/10.1016/S0040-1951(00)00150-5.

Korneva, I., Tondi, E., Jablonska, D., Di Celma, C., Alsop, I., Agosta, F., 2016. Distinguishing tectonically-and gravity-driven synsedimentary deformation structures along the Apulian platform margin (Gargano Promontory, southern Italy). Mar. Petrol. Geol. 73, 479–491.

La Bruna, V., Agosta, F., Lamarche, J., Viseur, S., Prosser, G., 2018. Fault growth mechanisms and scaling properties in foreland basin system: the case study of Monte Alpi, Southern Apennines, Italy. J. Struct. Geol. 116, 94–113. https://doi.org/10.1016/j.jsg.2018.08.009.

Lacombe, O., Malandain, J., Vilasi, N., Amrouch, K., Roure, F., 2009. From paleostresses to paleoburial in fold–thrust belts: preliminary results from calcite twin analysis in the Outer Albanides. Tectonophysics 475 (1), 128–141. https://doi.org/10.1016/j.tecto.2008.10.023.

Laj, C., Jamet, M., Sorel, D., Valente, J.P., 1982. First paleomagnetic results from Mio-Pliocene series of the Hellenic sedimentary arc. Tectonophysics 86 (1–3), 45–67. https://doi.org/10.1016/0040-1951(82)90061-0.

Lamarche, J., Lavenu, A.P.C., Gauthier, B.D.M., Guglielmi, Y., Jayet, O., 2012. Relationships between fracture patterns, geodynamics and mechanical stratigraphy in Carbonates (South-East Basin, France). Tectonophysics 581, 231–245. https://doi.org/10.1016/j.tecto.2012.06.042.

Lash, G.G., Engelder, T., 2007. Jointing within the outer arc of a forebulge at the onset of the Alleghanian Orogeny. J. Struct. Geol. 29 (5), 774–786. https://doi.org/10.1016/j.jsg.2006.12.002.

Laubach, S.E., 2003. Practical approaches to identifying sealed and open fractures. AAPG Bull. 87, 561–579. https://doi.org/10.1306/11060201106.

Laubach, S.E., Marrett, R.A., Olson, J.E., Scott, A.R., 1998. Characteristics and origins of coal cleat: a review. Int. J. Coal Geol. 35 (1–4), 175–207. https://doi.org/10.1016/S0166-5162(97)00012-8.

Le Pichon, X., Lybéris, N., Angelier, J., Renard, V., 1982. Strain distribution over the east Mediterranean ridge: a synthesis incorporating new Sea-Beam data. Tectonophysics 86 (1–3), 243–274. https://doi.org/10.1016/0040-1951(82)90069-5.

Louvari, E., Kiratzi, A.A., Papazachos, B.C., 1999. The Cephalonia transform fault and its extension to western Lefkada Island (Greece). Tectonophysics 308 (1–2), 223–236. https://doi.org/10.1016/S0040-1951(99)00078-5.

Marshak, S., 1988. Kinematics of orocline and arc formation in thin-skinned orogens. Tectonics 7 (1), 73–86. https://doi.org/10.1029/TC007i001p00073.

Marshak, S., 2004. Salients, recesses, arcs, Oroclines, and Syntaxes - a review of ideas concerning the formation of map-view curves in fold-thrust belts. AAPG Mem. 82, 131–156. https://doi.org/10.1306/M82813C9.

Mattei, M., Cifelli, F., Alimohammadian, H., Rashid, H., Winkler, A., Sagnotti, L., 2017. Oroclinal bending in the Alborz Mountains (northern Iran): new constraints on the age of south Caspian subduction and extrusion tectonics. Gondwana Res. 42, 13–28. https://doi.org/10.1016/j.gr.2016.10.003.

Mazzoli, S., Lanci, L., De Donatis, M., 2001. Paleomagnetic rotations in thrust belts: a case-study from the Marche-Romagna area (Northern Apennines, Italy). J. Geodyn. 32, 373–393.

Mazzoli, S., Pierantoni, P.P., Borraccini, F., Paltrinieri, W., Deiana, G., 2005. Geometry, segmentation pattern and displacement variations along a major Apennine thrust zone, central Italy. J. Struct. Geol. 27, 1940–1953.

McKenzie, D., 1972. Active tectonics of the Mediterranean region. Geophys. J. R. Astron. Soc. 30 (2), 109–185. https://doi.org/10.1111/j.1365-246X.1972.tb02351.x.

McKenzie, D., 1978. Active tectonics of the Alpine—Himalayan belt: the Aegean Sea and surrounding regions. Geophys. J. Int. 55 (1), 217–254. https://doi.org/10.1111/j.1365-246X.1978.tb04759.x.

Mitra, G., Yonkee, W.A., 1985. Relationship of spaced cleavage to folds and thrusts in the Idaho-Utah-Wyoming thrust belt. J. Struct. Geol. 7 (3–4), 361–373. https://doi.org/10.1016/0191-8141(85)90041-0.

Morris, A., Robertson, A.H.F., 1993. Miocene remagnetisation of carbonate platform and Antalya complex units within the Isparta angle, SW Turkey. Tectonophysics 220 (1–4), 243–266. https://doi.org/10.1016/0040-1951(93)90234-B.

Mountrakis, D., 1986. The Pelagonian zone in Greece: a polyphase-deformed fragment of the Cimmerian continent and its role in the geotectonic evolution of the eastern Mediterranean. J. Geol. 94 (3), 335–347. https://doi.org/10.1086/629033.

Muñoz, J.A., Beamud, E., Fernández, O., Arbués, P., Dinarès-Turell, J., Poblet, J., 2013. The Ainsa Fold and thrust oblique zone of the central Pyrenees: kinematics of a curved contractional system from paleomagnetic and structural data. Tectonics 32 (5), 1142–1175. https://doi.org/10.1002/tect.20070.

Papanikolaou, D., 2009. Timing of tectonic emplacement of the ophiolites and terrane paleogeography in the Hellenides. Lithos 108 (1–4), 262–280. https://doi.org/10.1016/j.lithos.2008.08.003.

Pastor-Galán, D., Gutiérrez-Alonso, G., Weil, A.B., 2011. Orocline timing through joint analysis: insights from the Ibero-Armorican arc. Tectonophysics 507 (1–4), 31–46. https://doi.org/10.1016/j.tecto.2011.05.005.

Pastor-Galán, D., Mulchrone, K.F., Koymans, M.R., van Hinsbergen, D.J., Langereis, C.G., 2017. Bootstrapped total least squares orocline test: a robust method to quantify vertical-axis rotation patterns in orogens, with examples from the Cantabrian and Aegean oroclines. Lithosphere 9 (3), 499–511. https://doi.org/10.1130/L547.1.

Pearce, F.D., Rondenay, S., Sachpazi, M., Charalampakis, M., Royden, L.H., 2012. Seismic investigation of the transition from continental to oceanic subduction along the western Hellenic Subduction Zone. J. Geophys. Res. Solid Earth 117 (B7). https://doi.org/10.1029/2011JB009023.

Pérouse, E., Sébrier, M., Braucher, R., Chamot-Rooke, N., Bourlès, D., Briole, P., Sorel, D., Dimitrov, D., Arsenikos, S., 2017. Transition from collision to subduction in Western Greece: the Katouna–Stamna active fault system and regional kinematics. Int. J. Earth Sci. 106 (3), 967–989. https://doi.org/10.1007/s00531-016-1345-9.

Quintà, A., Tavani, S., 2012. The foreland deformation in the south-western Basque–Cantabrian Belt (Spain). Tectonophysics 576, 4–19. https://doi.org/10.1016/j.tecto.2012.02.015.

Railsback, L.B., Andrews, L.M., 1995. Tectonic stylolites in the 'undeformed'Cumberland Plateau of southern Tennessee. J. Struct. Geol. 17 (6), 911–915. https://doi.org/10.1016/0191-8141(94)00127-L.

Rawnsley, K.D., Peacock, D.C.P., Rives, T., Petit, J.-P., 1998. Joints in the mesozoic sediments around the Bristol channel basin. J. Struct. Geol. 20, 1641–1661.

Renz, C., 1955. Die vorneogene stratigraphie der normal-sedimentaren formationen Griechenlands. Institute of Geological Subsurface Research, Athens, pp. 637.

Ries, A.C., Shackleton, R.M., 1976. Patterns of strain variation in arcuate fold belts. Philos. Trans. R. Soc. Lond. Pt. A 283, 281–288. https://doi.org/10.1098/rsta.1976.0085.

Robertson, A.H.F., Dixon, J.E., 1984. Introduction: aspects of the geological evolution of the Eastern Mediterranean. Geol. Soc. Lond. Spec. Publ. 17 (1), 1–74. https://doi.org/10.1144/GSL.SP.1984.017.01.02.

Robertson, A.H.F., Shallo, M., 2000. Mesozoic–Tertiary tectonic evolution of Albania in its regional Eastern Mediterranean context. Tectonophysics 316 (3–4), 197–254. https://doi.org/10.1016/S0040-1951(99)00262-0.

Robertson, A.H.F., Clift, P.D., Degnan, P.J., Jones, G., 1991. Palaeogeographic and palaeotectonic evolution of the eastern Mediterranean Neotethys. Palaeogeogr. Palaeoclimatol. Palaeoecol. 87 (1–4), 289–343. https://doi.org/10.1016/0031-0182(91)90140-M.

Rosenbaum, G., 2014. Geodynamics of oroclinal bending: insights from the Mediterranean. J. Geodyn. 82, 5–15. https://doi.org/10.1016/j.jog.2014.05.002.

Roure, F., Nazaj, S., Mushka, K., Fili, I., Cadet, J.P., Bonneau, M., 2004. Kinematic evolution and petroleum systems: an appraisal of the outer Albanides. Thrust Tecton. Hydrocarbon Syst. 82 474–49.
Rustichelli, A., Torrieri, S., Tondi, E., Laurita, S., Strauss, C., Agosta, F., Balsamo, F., 2016. Fracture characteristics in Cretaceous platform and overlying ramp carbonates: an outcrop study from Maiella Mountain (central Italy). Mar. Petrol. Geol. 76, 68–87.
Saccani, E., Padoa, E., Photiades, A., 2003. Triassic mid-ocean ridge basalts from the Argolis Peninsula (Greece): new constraints for the early oceanization phases of the Neo-Tethyan Pindos basin. Geol. Soc. Lond. Spec. Publ. 218 (1), 109–127. https://doi.org/10.1144/GSL.SP.2003.218.01.07.
Sachpazi, M., Hirn, A., Clément, C., Haslinger, F., Laigle, M., Kissling, E., Charvis, P., Hello, Y., Lépine, J.C., Sapin, M., Ansorge, J., 2000. Western Hellenic subduction and Cephalonia Transform: local earthquakes and plate transport and strain. Tectonophysics 319 (4), 301–319. https://doi.org/10.1016/S0040-1951(99)00300-5.
Salvini, F., Vittori, E., 1982. Analisi strutturale della linea Olevano-Antrodoco-Posta (Ancona-Anzio Auct.); metodologia di studio delle deformazioni fragili e presentazione del tratto meridionale. Memor. Soc. Geol. Ital. 24, 337–355.
Savignano, E., Mazzoli, S., Arce, M., Franchini, M., Gautheron, C., Paolini, M., Zattin, M., 2016. (Un)Coupled thrust belt-foreland deformation in the northern Patagonian Andes: new insights from the Esquel-Gastre sector (41°30′–43°S). Tectonics 35, 2636–2656. https://doi.org/10.1002/2016TC004225.
Silver, E.A., Reed, D.L., Tagudin, J.E., Heil, D.J., 1990. Implications of the north and south Panama thrust belts for the origin of the Panama orocline. Tectonics 9 (2), 261–281. https://doi.org/10.1029/TC009i002p00261.
Skourlis, K., Doutsos, T., 2003. The Pindos Fold and Thrust Belt (Greece): inversion kinematics of a passive continental margin. Int. J. Earth Sci. 92, 891–903. https://doi.org/10.1007/s00531-003-0365-4.
Skourtsis-Coroneou, V., Solakius, N., Constantinidis, I., 1995. Cretaceous stratigraphy of the Ionian zone, Hellenides, western Greece. Cretac. Res. 16 (5), 539–558. https://doi.org/10.1006/cres.1995.1035.
Smith, A.G., Moores, E.M., 1974. Hellenides. Geol. Soc. Lond. Spec. Publ. 4 (1), 159–185. https://doi.org/10.1144/GSL.SP.2005.004.01.09.
Smith, A.G., Woodcock, N.H., Naylor, M.A., 1979. The structural evolution of a Mesozoic continental margin, Othris Mountains, Greece. J. Geol. Soc. 136 (5), 589–601. https://doi.org/10.1144/gsjgs.136.5.0589.
Sotiropoulos, S., Kamberis, E., Triantaphyllou, M.V., Doutsos, T., 2003. Thrust sequences in the central part of the External Hellenides. Geol. Mag. 140 (6), 661–668. https://doi.org/10.1017/S0016756803008367.
Sotiropoulos, S., Triantaphyllou, M.V., Kamberis, E., Tsaila-Monopolis, S., 2008. Paleogene terrigenous (flysch) sequences in Etoloakarnania region (w. Greece). Plankton stratigraphy and paleoenvironmental implications. Geobios 41, 415–433. https://doi.org/10.1016/j.geobios.2007.10.007.
Spakman, W., Wortel, M.J.R., Vlaar, N.J., 1988. The Hellenic subduction zone: a tomographic image and its geodynamic implications. Geophys. Res. Lett. 15 (1), 60–63. https://doi.org/10.1029/GL015i001p00060.
Speranza, F., Islami, I., Kissel, C., Hyseni, A., 1995. Paleomagnetic evidence for Cenozoic clockwise rotation of the external Albanides. Earth Planet. Sci. Lett. 129 (1–4), 121–134. https://doi.org/10.1016/0012-821X(94)00231-M.
Speranza, F., Sagnotti, L., Mattei, M., 1997. Tectonics of the Umbria-Marche-Romagna arc (central northern Apennines, Italy): new paleomagnetic constraints. J. Geophys. Res. Solid Earth 102 (B2), 3153–3166. https://doi.org/10.1029/96JB03116.
Stearns, D.W., 1968. Certain aspects of fractures in naturally deformed rocks. In: Riecker, R.E. (Ed.), Rock Mechanics Seminar: Bedford. Terrestrial Sciences Laboratory, pp. 97–118.
Szaniawski, R., Mazzoli, S., Jankowski, L., 2017. Controls of structural inheritance on orogenic curvature and foreland basin sedimentation: insights from the Przemyśl area, Western Carpathians. J. Struct. Geol. 103, 137–150. https://doi.org/10.1016/j.jsg.2017.09.004.
Tavani, S., Storti, F., Bausà, J., Muñoz, J.A., 2012. Late thrusting extensional collapse at the mountain front of the northern Apennines (Italy). Tectonics 31 (4), TC4019. https://doi.org/10.1029/2011TC003059.
Tavani, S., Storti, F., Lacombe, O., Corradetti, A., Muñoz, J.A., Mazzoli, S., 2015. A review of deformation pattern templates in foreland basin systems and fold-and-thrust belts: implications for the state of stress in the frontal regions of thrust wedges. Earth Sci. Rev. 141, 82–104. https://doi.org/10.1016/j.earscirev.2014.11.013.
Tavani, S., Corradetti, A., Sabbatino, M., Morsalnejad, D., Mazzoli, S., 2018. The Meso-Cenozoic fracture pattern of the Lurestan region, Iran: the role of rifting, convergence, and differential compaction in the development of pre-orogenic oblique fractures in the Zagros Belt. Tectonophysics 749, 104–119. https://doi.org/10.1016/j.tecto.2018.10.031.
Tavarnelli, E., 1997. Structural evolution of a foreland fold-and-thrust belt: the Umbria-Marche Apennines, Italy. J. Struct. Geol. 19 (3–4), 523–534. https://doi.org/10.1016/S0191-8141(96)00093-4.
Triantaphyllou, M.V., 2013. Calcareous nannofossil dating of Ionian and Gavrovo flysch deposits in the external Hellenides carbonate platform (Greece): overview and implications. Tectonophysics 595–596, 235–249. https://doi.org/10.1016/j.tecto.2012.05.007.
Ukar, E., Laubach, S.E., Hooker, J.N., 2019. Outcrops as guides to subsurface natural fractures: example from the Nikanassin Formation tight-gas sandstone, Grande Cache, Alberta foothills, Canada. Mar. Petrol. Geol. 103, 255–275. https://doi.org/10.1016/j.marpetgeo.2019.01.039.
Underhill, J.R., 1988. Triassic evaporites and Plio-Quaternary diapirism in western Greece. J. Geol. Soc. 145 (2), 269–282. https://doi.org/10.1144/gsjgs.145.2.0269.
Underhill, J.R., 1989. Late Cenozoic deformation of the Hellenide foreland, western Greece. Geol. Soc. Am. Bull. 101 (5), 613–634. https://doi.org/10.1130/0016-7606(1989)101%3C0613:LCDOTH%3E2.3.CO;2.
van Hinsbergen, D.J.J., Langereis, C.G., Meulenkamp, J.E., 2005. Revision of the timing, magnitude and distribution of Neogene rotations in the western Aegean region. Tectonophysics 396, 1–34. https://doi.org/10.1016/j.tecto.2004.10.001.
van Hinsbergen, D.J.J., van der Meer, D.G., Zachariasse, W.J., Meulenkamp, J.E., 2006. Deformation of western Greece during Neogene clockwise rotation and collision with Apulia. Int. J. Earth Sci. 95 (3), 463. https://doi.org/10.1007/s00531-005-0047-5.
van Hinsbergen, D.J.J., Dekkers, M.J., Koç, A., 2010. Testing Miocene remagnetization of Bey Dağları: timing and amount of neogene rotations in SW Turkey. Turk. J. Earth Sci. 19, 123–156 10 .3906/yer-0904-1.
Vidal-Royo, O., Koyi, H.A., Muñoz, J.A., 2009. Formation of orogen-perpendicular thrusts due to mechanical contrasts in the basal décollement in the Central External Sierras (Southern Pyrenees, Spain). J. Struct. Geol. 31 (5), 523–539. https://doi.org/10.1016/j.jsg.2009.03.011.
Weil, A.B., Sussman, A.J., 2004. Classifying curved orogens based on timing relationships between structural development and vertical-axis rotations. In: Orogenic Curvature: Integrating Paleomagnetic and Structural Analyses. Geological Society of America, vol. 383. pp. 1–15.
Weil, A.B., Yonkee, W.A., 2012. Layer-parallel shortening across the Sevier fold-thrust belt and Laramide foreland of Wyoming: spatial and temporal evolution of a complex geodynamic system. Earth Planet. Sci. Lett. 357, 405–420. https://doi.org/10.1016/j.epsl.2012.09.021.
Weil, A.B., Van der Voo, R., Van der Pluijm, B.A., Parés, J.M., 2000. The formation of an orocline by multiphase deformation: a paleomagnetic investigation of the Cantabria–Asturias Arc (northern Spain). J. Struct. Geol. 22 (6), 735–756. https://doi.org/10.1016/S0191-8141(99)00188-1.
Weil, A.B., Gutiérrez-Alonso, G., Johnston, S.T., Pastor-Galán, D., 2013. Kinematic constraints on buckling a lithospheric-scale orocline along the northern margin of Gondwana: a geologic synthesis. Tectonophysics 582, 25–49. https://doi.org/10.1016/j.tecto.2012.10.006.
Zhou, X., Aydin, A., 2012. Mechanics of the formation of orthogonal sets of solution seams, and solution seams and veins and parallel solution seams and veins. Tectonophysics 532, 242–257. https://doi.org/10.1016/j.tecto.2012.02.013.